

Final Report

Project Title: Technology and Enhancements to Improve Pre-Crash Safety

September 30, 2018

Submitted to: US Department of Transportation (USDOT)
Research and Innovation Technology Administration (RITA)

Program Director/PI: Umit Ozguner
Crash Imminent Safety University Transportation Center Director
Professor Emeritus
TRC Inc. Chair on Intelligent Transportation Systems
Department of Electrical and Computer Engineering
The Ohio State University
ozguner.1@osu.edu
614-292-5141

Project Lead: Umit Ozguner, The Ohio State University
ozguner.1@osu.edu, 614-292-5141

Participating: Y. Chen (IUPUI); B. Coifman (OSU); A. Homaifar (NCA&T); E. Ekici (OSU); F. Ozguner (OSU); K. Redmill (OSU); Zheng (IUPUI); E. Koksal (OSU)

DUNS Number: 832127323, EIN Number: 31-6025986

Recipient Organization: The Ohio State University

Recipient Grant Number: DTRT13-G-UTC47

Project/Grant Period: 10/01/2013-09/30/2018

Submission Date: 09/30/2018

Signature of Submitting Official:



DISCLAIMER

The contents of this report reflect the views of the authors, who are responsible for the facts and the accuracy of the information presented herein. This document is disseminated under the sponsorship of the U.S. Department of Transportation's University Transportation Centers Program, in the interest of information exchange. The U.S. Government assumes no liability for the contents or use thereof.

OVERVIEW

This is the Final Report of the Project

Technology and Enhancements to Improve Pre-Crash Safety

Project Lead: Umit Ozguner

Director, University Transportation Center (UTC)
Professor, Department of Electrical & Computer Engineering
Transportation Research Center (TRC) Inc. Chair on Intelligent Transportation Systems (ITS)
Email: ozguner.1@osu.edu
Office: 614-292-5940 Fax: 614-292-7596
205 Dreese Laboratories; 2015 Neil Avenue, Columbus OH, 43210

Other Investigators: Yaobin Chen (IUPUI), Eylem Ekici (OSU), Fusun Ozguner (OSU), Keith Redmill (OSU)

Project Descriptions

This Project was a combination of multiple smaller, short-term sub-projects under the general theme of “Technology and Enhancements to Improve Pre-Crash Safety”. It focuses on technology improvements that can be implemented in intelligent and autonomous vehicles toward the goal of improving pre-crash safety.

EEG and Lane Change Intent Evaluation on a Driving Simulator

With autonomous vehicles being on the verge of deployment as part of city infrastructure, the need for autonomous vehicles to be capable of anticipating human driver intent is inescapable. Newer technologies and potentially controversial sensing options, such as gaze direction, driver body language/weight shifting, and even electroencephalogram (EEG) sensors, are available for exploration. Recent research has shown the crucial importance of gaze monitoring. For example, on the approach to curves, driver gaze direction can predict speed at the apex and crashes. Drivers’ gaze duration on external signs can predict their ability to keep in their lane. We propose to explore technologies for sensing driver attention and their impact in pre-crash scenarios. In conjunction with Project 1, we will design and test biomonitors and their value in improving crash safety. We will also predict, using behavior models, the extent to which monitoring information can be effective in improving pre-crash safety.

Cognitive Radio Based Communication

In this sub-project, we study the value of V2I and V2V communications for improving pre-crash safety. Using simulator studies—and later, field tests for promising approaches—we will study scenarios in which location and heading information for nearby vehicles is used, and we will test its value in averting crashes or minimizing crash injury. An important element of this understanding is how the (in)accuracy of this information impacts safety performance. V2V hardware testing facilities in OSU’s Control and Intelligent Transportations Research (CITR) Laboratory will be used to quantify location accuracy in realistic scenarios. We will also study information accuracy as it impacts information trust in the corresponding behavioral models being developed in Project 3.

Secure, Privacy-preserving, and Efficient Communication Framework to Support Crash-Imminent Safety Situations

In this sub-project we study the impact of both intra-vehicle and inter-vehicle communication cybersecurity on pre-crash scenarios. A number of issues are of concern: external “snooping”; injection of false information externally; and “hacking” the vehicular software. Several countermeasures are being developed, including key generation and filtering. Our focus in the CrIS UTC will be on the implications of cyber-threats on pre-crash safety. For example, cybersecurity countermeasures result in data latency; we will investigate how this latency degrades safety margins. As a second example, inaccurate information, including false warning indicators that may result from either compromised security or communication noise reduce driver trust in the data, and result in a change of driver behavior in response to these indicators.

Analyzing and Mining Big Data of Driving Videos for Crash Avoidance

The purpose of this project is to construct an online video database to host big data of naturalistic driving video including crash and near miss cases from recent populated vehicle borne cameras for accident verification and the crash avoidance technology development. A series of new video processing methods is developed for large-scale driving video indexing, browsing, visualization, automatic event detection, and accurate measuring of vehicle and environmental parameters in the videos. Big Data mining is applied to summarizing parameter distributions for extracting critical factors of crash in the video dataset. The video and data have been uploaded for analyzing accidents and surveying results for the design of vehicle safety functions and crash testing scenarios.

CAAIS: Context-Aware Authentication Interchange Scheme in Vehicular Networks

Any cutting-edge technology, such as Internet of things, cyber physical systems, big data, or cloud computing, necessitates a security measure to afford trustability. Existing standards and specifications recommend the use of a state-of-the-art cryptographic Public Key Infrastructure (PKI) framework. PKI utilizes the public key encryption and digital signatures to meet the three main requirements of a secure system: authentication of system users, integrity of exchanged information, and that originators of information cannot repudiate their generation of data. However, in some types of such innovative technologies, PKI could have limitations. One such context is when using PKI to secure communications in vehicular networks.

Safety Implications of Traffic Dynamics in Congested Freeway Traffic

This research has focused on driver behavior in the presence of large speed differentials between lanes. Results have found that drivers' car-following behavior not only depends on the lead vehicle in their lane, but also the speed of the adjacent lane. It turns out that these dependencies can also emerge in seemingly free flow traffic. Specifically, when traveling next to a slow-moving lane some drivers will choose a free speed below the speed limit. This new-found regime will help advance our understanding of how congested traffic can really a mix of queued and non-queued traffic, and thus, having the potential to exhibit properties of both states.

Smart Cities: A Simple Framework for On-Demand Mobility Services

An effort was undertaken to develop slow-moving platforms (single-person or 4-people vehicles) that would provide transportation for the mobility-impaired in a smart city. The effort has been initiated by the City of Columbus and later supported by an NSF Project (through its CPS: Smart Cities Program). Within this small sub-

project we investigated the computer-communication architecture needed to establish such a service and considered the “crash imminent” situations between pedestrians and vehicles.

Secure, Privacy-preserving, and Efficient Communication Framework to Support Crash-Imminent Safety Situations

Sub-Project PI: Prof. Fusun Ozguner

Dept. of ECE

Ohio State University

Secure, Privacy-preserving, and Efficient Communication Framework to Support Crash-Imminent Safety Situations

In this project we undertake multiple *Sub-Topics*, each concentrating on a different new technology that may have an effect in improving pre-crash safety.

Accomplishments: Throughout the last years, our main focus has been on investigating algorithms and approaches to secure, preserve privacy, and enhance efficiency of the vehicular communications. Our developed approaches overcome the shortcomings of the adopted Public Key Infrastructure (PKI) framework in the Dedicated Short-Range Communications (DSRC) suite of standards. Besides our previous confidentiality and secrecy of communication research, during the last six months, we have continued tackling the:

1. **Preserving Location-privacy of Vehicles.** We propose a scheme to hide the changing of certificates/pseudonyms in PKI to prevent eavesdroppers from easily linking the used single pseudonym with the vehicle's identity. The idea is to have vehicles create dynamic mix zones using an alternative super anonymous authentication scheme to hide their pseudonym change. Once the change occurs, the originating vehicle watches for at least one other alteration by any cooperative neighbor in the formed zone before the vehicle automatically demolishes the group by reverting back to the baseline authentication. The numerical evaluation of our scheme shows its effectiveness and how it gives comparable performance to that of the basic authentication in terms of computation time, storage cost, and number of vehicles.
2. **Efficiency of vehicular communications.** To overcome the heavy authentication load on the wireless medium the inefficiency of the adopted Carrier Sense Medium Access with Collision Avoidance (CSMA/CA) schemes in dense scenarios, our second track of research focuses on building a new cooperative beaconing strategy: Grouping for Beaconing Efficiency Enhancement (G-BEE). We use the concept of grouping to offload the main load of Vehicle-to-Infrastructure (V2I) beaconing from all network users to only group leaders. This transforms the problem of medium access from a dense network of short sessions into one with a sparse network of longer sessions, the ideal setting for CSMA/CA. We introduce two versions of G-BEE: simple and enhanced to deal with two levels of authentication-overhead omission. We investigate the gain of our strategies by building stochastic analytical models. The numerical evaluations show that both G-BEE versions outperform the classical individual scenario and achieve higher gains in terms of maximum number of vehicles, delay rate, collision rate, drop rate, and throughput metrics.

Products: Publications:

1. S. Al-Shareeda and F. Özgüner, "Preserving location privacy using an anonymous authentication dynamic mixing crowd," in proceedings of the IEEE 19th International Conference on Intelligent Transportation Systems (ITSC2016), pp. 545-550, 2016.
2. Y. Feng, S. Al-Shareeda, C. Emre Koksal, and F. Özgüner, "G-BEE: Grouping for Beaconing Efficiency Enhancement in vehicular networks", submitted to the IEEE Transactions on Mobile Computing, 2017.

CAAIS: Context-Aware Authentication Interchange Scheme in Vehicular Networks

Sarah Al-Shareeda and Fusun Ozguner

Introduction

Any cutting-edge technology, such as Internet of things, cyber physical systems, big data, or cloud computing, necessitates a security measure to afford trustability. Existing standards and specifications recommend the use of

a state-of-the-art cryptographic Public Key Infrastructure (PKI) framework. PKI utilizes the public key encryption and digital signatures to meet the three main requirements of a secure system: authentication of system users, integrity of exchanged information, and that originators of information cannot repudiate their generation of data¹. However, in some types of such innovative technologies, PKI could have limitations. One such context is when using PKI to secure communications in **vehicular networks**².

Motivation: PKI Shortcomings in the Context of Vehicular Communications

“Vehicles talk to each other” is a buzzword we are hearing nowadays. It is not a far-reaching goal; the development of the Dedicated Short-Range Communication (DSRC) standard in the US and the Cooperative - Intelligent Transport Systems (C-ITS) in Europe make this objective a reality. When focusing on how these standards will secure vehicular communications, we see that both standards adopt the PKI framework to safeguard the vehicles under the project of Security Credential Management System (SCMS) that is in its proof of concept (PoC) phase^{2,3,4}. To make the concept easier to understand, we delineate the vehicular system’s actors and actions below:

Actors: Trusted Authority (TA), Vehicles, On Board Unit (OBU), Road Side Unit (RSU), and Attackers

Actions: Vehicles register with TA, Vehicles broadcast their beacons, Vehicles sign outgoing beacons, and Vehicles verify received beacons

Links: Vehicle-to-Vehicle (V2V), Vehicle-to-Infrastructure (V2I), Infrastructure-to- Vehicle (I2V), and Vehicle-to-Everything (V2X)

A typical vehicular system model is shown in Figure 1; each vehicle is given an OBU to store any given parameters at time of registration with the TA. RSUs represent the infrastructure with which the vehicles will communicate after deployment.

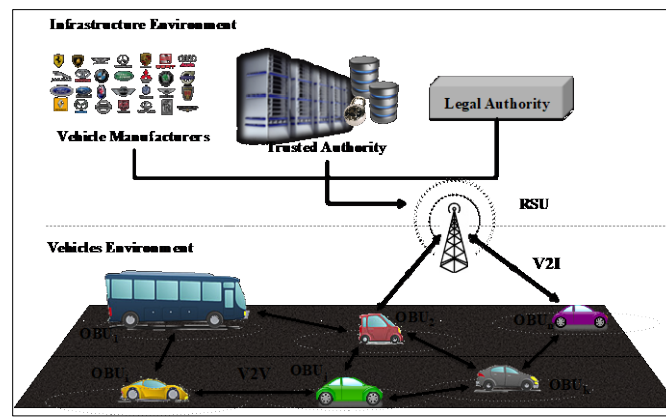


Figure 1 Typical Vehicular Network

At the outset, in PKI, the TA or Certification Authority (CA) has an identity ID_{CA} , a secret key sk_{CA} , and a public key pk_{CA} . By giving its electronic license plate number to the CA, vehicle v obtains the CA’s public key pk_{CA} , a long-term identity ID_v that has no public relationship with the auto’s electronic license plate number, and a certified long-term (sk_{CA}, pk_{CA}) key pair. In this way, CA keeps record of every registered vehicle and its assigned credentials, so whenever a vehicle misbehaves or is compromised, CA adds it to a Certificate Revocation

¹ https://en.wikipedia.org/wiki/Public_key_infrastructure

² Maxim Raya and Jean Pierre Hubaux. The security of vehicular ad hoc networks. In the 3rd ACM workshop on Security of ad hoc and sensor networks, ACM, pp. 11-21, 2005.

³ John B Kenney, Dedicated short-range communications (DSRC) standards in the United States, IEEE, 99(7): 1162-1182, 2011.

⁴ <https://wiki.campllc.org/display/SCP/SCMS+CV+Pilots+Documentation>

List (CRL) list that is periodically broadcasted by the infrastructure RSUs to the members of the network. When deployed, autos will periodically broadcast safety messages m_v to inform neighbors about their current status. The beaconing rate mainly pertains to the GPS frequency and synchronization interval of DSRC. Whenever v wants to broadcast m_v , v digitally signs the concatenation of a hashed m_v with a fresh timestamp T_v (to avoid replay attacks) using sk_v before sending m_v with the related pk_v 's certificate; the format of the broadcasted m_v is:

$$m_v, sig_{sk_v}(h(m_v)|T_v), cer_{CA}(pk_v), \quad (1)$$

where:

$$cer_{CA}(pk_v) = pk_v | sig_{sk_{CA}}(pk_v | ID_{CA}). \quad (2)$$

Receiving (1), w or any RSU will only be able to verify (1) if it belongs to the network, i.e., it has the pk_{CA} . First, w finds whether the received pk_v is a revoked key by checking it against the contained CRL. If it is not revoked, w validates the signature and accepts m_v only if its hashed value equals the received digest $h(m_v)$ ⁵. For the integrity of the data, DSRC recommends the Secure Hash Algorithm (SHA)-2 family of hash functions, specifically SHA-256 that produces 256 bit message digests⁶. PKI fulfils the three main requirements of security: authentication, integrity, and non-repudiation as in Animation 1 (https://drive.google.com/open?id=1qAxE9_B9_t2lJb8KdaHmf795-TOn5mZY).

- Authentication: The security comes from the fact that only members who belong and register with the network obtain the public key (pk_{CA}) of CA. This fulfils the authentication requirement: senders are sure that no outsider can obtain their own keys and receivers who do not belong to the network cannot know the senders keys.
- Non-repudiation: Since the sender sends his public key to be used to verify his signature on his secret key, the non-denial is achieved; the sender cannot deny he sent the message since his secret key was used to create the signature.
- Integrity: to ensure that the sent message has not been altered, integrity is achieved via the use of hash function.

However, PKI alone cannot comprehensively meet all of the security and privacy requirements; **PKI has a large security payload to be attached with each broadcasted message and PKI cannot prevent eavesdroppers from tracking vehicles (as we'll see below) leading to location privacy deprivation.** Adding to this, the standards' Medium Access Control (MAC) layer adopts the IEEE 802.11p access mode, which also needs augmentation to fulfil the efficiency of communication when collisions arise for safety beacons. Since many issues have not been well addressed in DSRC/C-ITS, we have been incentivized to contribute with our own solution.

Objectives

The objective of our contribution is twofold:

1. Since some frameworks have small communication overhead while others have high anonymous traits, we developed an efficient identity based cryptographic alternative authentication for V2X with lower communication overhead. The built framework has fast computations, no elliptic curves pairings, smaller communication overhead, and more anonymous pseudo identities to achieve the needed privacy.

⁵ C. Paar and J. Pelzl, Understanding cryptography: a textbook for students and practitioners. Springer Science & Business Media, 2009.

⁶ John B Kenney, Dedicated short-range communications (DSRC) standards in the United States, IEEE, 99(7): 1162-1182, 2011.

2. As in Animation 1 (https://drive.google.com/open?id=1rRvJXzHIFsWu_Pia_r57Tt3NHoSI4e3I), our scheme has four phases: generate elliptic curve parameters at a central authority, register and obtain authentication parameters such as pseudo keys and identities by vehicles, online signing the broadcasted messages by senders, and online verification of received beacons by receivers. Our scheme does not rely on the certificates of PKI nor on the bilinear pairing of identity-based framework. Since the scheme eliminates the need for bilinear pairing, it conducts fewer computations in comparison with the available pairing based schemes.
3. Focusing on the efficiency aspect of vehicular communication, rather than using only PKI to authenticate users, a context aware authentication interchange protocol was introduced to match the situational neighborhood conditions of vehicles. We introduced an authentication interchange scheme that intermingles between three frameworks: PKI, group signature, and our new developed Identity-based Cryptographic (IBC) authentication. Every certain time interval, the PKI vehicle checks its context; if the vehicle encounters a crowded neighborhood, it switches to a lower-overhead IBC authentication. If the car's context is sparse, it alters to a more anonymous group signature framework as in Animation 2
4. (<https://drive.google.com/open?id=13K4mRHvfjkxHuHD76RQUAVQmntpOfeXp>).

After deployment, the vehicles are assumed to start with the PKI security framework where they periodically change their short-lived certificated pseudonyms to deceive eavesdroppers. The cars are given cryptographic ingredients of the three authentication schemes: PKI, GS, and IBC. Besides, to fulfil the needs of our proposal, any vehicle v is assumed to have:

- A Context Timer T_{Cv} that when it times out, v checks its surrounding context. We choose to set the initial value of T_{Cv} in compliance with the settings of DSRC specifications⁷. If we follow the adopted PKI framework specifications, we can make T_{Cv} hit zero every pseudonym lifetime, i.e., every 60 seconds. Also, we can relate the value of T_{Cv} with the distance v travels. If v travels at 112 km/h on US highways, a PKI beacon of a 310 byte, transferred at 6 Mbps rate, needs 0.414 msec to reach the receiver ignoring any medium access contention. Adding the signing and verifying computation costs of 5 msec, each beacon needs a 5.414 msec communication time. For both ends of communication, per a total time of 10.8 msec, v is moving only 0.336 m. If v wants to examine its context every 10 m, T_{Cv} can be set to 322.8 msec.
- To illustrate vehicle v 's surrounding context, we assume the availability of a
 - o Number of Neighbors Counter N_{Cv} : also, N_{Cv} can refer to the number of beacons that v receives during its context timer interval T_{Cv} . We initialize it to >1 value and after deployment it is incremented with every received beacon. If N_{Cv} becomes larger than a specific threshold $\xi_{N_{Cv}}$, v has to switch to a lighter-weight authentication such as our new IBC scheme. If N_{Cv} is small, v can accommodate heavy-weight authentications such as PKI and even GS.
 - o Vehicle Anonymity A_v : in our settings, vehicle anonymity is interpreted in the terms of the total entropy of the received beacons within the T_{Cv} context timer interval as $A_v(T_{Cv}) = \frac{\sum_{i=0}^{N_{Cv}} pg_v^i \cdot \text{Log}(\frac{1}{pg_v^i})}{\text{Log}(N_{Cv})}$, where the power gain pg_v^i , between vehicles v and i , refers to the signal strength of the received

⁷ John B Kenney, Dedicated short-range communications (DSRC) standards in the United States, IEEE, 99(7): 1162-1182, 2011.

beacon from i by v within the T_{C_v} time interval. We assume pg_v^i to be normalized within the $[0, 1]$ range and A_v 's initial value is obtained after a single beacon interval of $T=100$ msec elapsed. Also, N_{C_v} has to be >1 to eliminate dividing by zero case. The value of A_v increases by the growth of the number of neighbors. When the number of neighbors or received beacons is small and is under a designated threshold ξ_{A_v} , v has to switch to a more anonymous authentication such as group signature authentication; once N_{C_v} starts growing, the risk is lifted since v will achieve better than ξ_{A_v} and v can switch to another anonymous authentication that does not need to be super anonymous.

- Maximum Tolerated Communication Overhead C_{O_v} : is the multiplication of the allowed number of vehicles in the network and the broadcasted beacon size. C_{O_v} increases either when beacon size is large or more vehicles are presented in the network. However, due to the limited CCH 46 msec width, the number of vehicles that can capture the wireless medium is limited; therefore, the increment of the C_{O_v} is caused by larger beacon sizes, i.e., type of authentication scheme. By developing CAAIS, we want to keep C_{O_v} within a fixed limit $\xi_{C_{O_v}}$; we achieve this by letting the vehicles change their authentication to the lighter IBC framework when the $\xi_{C_{O_v}}$ threshold is reached; otherwise, each v has the freedom to use any authentication. As with A_v , the initial value of C_{O_v} is decided after the elapse of one T beacon interval.

The values of the assigned thresholds $\langle \xi_{N_{C_v}}, \xi_{A_v}, \xi_{C_{O_v}} \rangle$ have to be carefully chosen in accordance with existing DSRC specifications and our own design preference.

To fully and comprehensively describe the CAAIS approach, we illustrate two scenarios in which vehicle v can call the CAAIS authentication interchange procedure depending on the current status of v 's surrounding context. The initial values of these three context parameters are decided before deployment. After deployment, they are updated with every arrival of a new beacon from neighbouring vehicles and infrastructure. Since the beacons are periodically broadcasted every T seconds, their arrival rates to v are deterministic and equal T . Also, we assume the number of cars in v 's context to be random but does not exceed the limit we set, then the total number of beacons received per second will be $N_{C_v} \times T$. Moreover, the obtained signal strength pg_v^i of the received beacon will be normalized to random probability values between 0 and 1; pg_v^i contributes to the accumulated degree of anonymity A_v . When T_{C_v} times out, the updated $\langle N_{C_v}, A_v, C_{O_v} \rangle$ parameters are compared to the assigned thresholds; v decides to keep its current authentication or to change to an alternative framework depending on the result of the considered comparison.

CAAIS Without Grouping Scenario: in this first scenario, a general simple case is discussed; all vehicles in the network are assumed to be individuals, i.e., no groups/clusters/zones are formed and all vehicles' beacons have the same priority. The considered comparison starts after updating all context parameters values and T_{C_v} timed out. If the number of neighbors N_{C_v} is greater than the designated threshold, v switches to the light-weight IBC authentication to relax the overall network overhead. Otherwise, if the number of vehicles still within limits, the algorithm checks the total communication overhead C_{O_v} in the network from v 's point of view; if there is greater than the assigned threshold, the vehicle keeps its PKI authentication; otherwise, v has to decide to switch to GS framework if the obtained degree of anonymity A_v is very low (this means that v 's

context is very scarce) or v keeps its PKI framework. We also give a simple illustrative example in the following table where v has three different cases of changing context. For $\xi_{N_{C_v}} = 4$, $\xi_{A_v} = 4$, and $\xi_{C_{O_v}} = 0.8 \times \xi_{N_{C_v}} \times beacon_{size}(GS)$, v will decide to switch to which authentication scheme. When the number of neighbour is $7 > \xi_{N_{C_v}} 7$, v chooses our new IBC framework. When $N_{C_v} = \xi_{N_{C_v}} = 4$, v checks the communication overhead and anonymity value and decides to keep its PKI authentication. When the obtained anonymity degree is so low when $N_{C_v} = 2$, v has to have more private atmosphere and this can be only achieved by switching to the super anonymous GS authentication.

Table 1: Three Cases of Context Changing Around Vehicle v

N_{C_v}	2	7	4
A_v	$\frac{\sum_{i=1}^2 (pg_v^i \cdot \text{Log}(\frac{1}{pg_v^i}))}{\text{Log}(2)}$	$\frac{\sum_{i=1}^7 (pg_v^i \cdot \text{Log}(\frac{1}{pg_v^i}))}{\text{Log}(7)}$	$\frac{\sum_{i=1}^4 (pg_v^i \cdot \text{Log}(\frac{1}{pg_v^i}))}{\text{Log}(4)}$
C_{O_v}	$C_{O_v, in} + (N_{C_v} * Beacon\ Size)$		
Authentication	$(N_{C_v} < \xi_{N_{C_v}}) \wedge (C_{O_v} < \xi_{C_{O_v}}) \wedge (A_v < \xi_{A_v}) \rightarrow GS$	$N_{C_v} > \xi_{N_{C_v}} \rightarrow IBC$	$(N_{C_v} = \xi_{N_{C_v}}) \wedge (C_{O_v} < \xi_{C_{O_v}}) \wedge (A_v > \xi_{A_v}) \rightarrow PKI$

CAAIS With Clustering Scenario: in this setup, vehicles can be either leaders CL whose beacons have higher priority to be sent on the wireless medium or members CM of groups. The leadership and membership roles are decided after deployment. However, before deployment, each vehicle v is assumed to be a single cluster leader CL of a Cluster Size S_{C_v} parameter equals 1. Despite of being cooperative and preferring to have larger S_{C_v} size, v is given a specific threshold $\xi_{S_{C_v}}$ of its cluster size. Also, each v will have a Number of Leaders parameter N_{L_v} with threshold $\xi_{N_{L_v}}$ and Cluster Members Set CMS_v that has the form of

$CMS_v = [CL_{v_{info}}, CM_{1_{\Delta CL_{info}}}, \dots]$. CMS_v includes the information of the cluster leader (its current hashed alias identity, current location, current speed, current direction, etc.) as well as the relative information of all members in this CL cluster. The CMS_v initial value is one of the hashed alias identities that was given to v as part of the IBC authentication. When new vehicles are joining the cluster, the set is updated with the pseudo identities of the joined members. These new parameters are given to v besides the cryptographic parameters of three authentication frameworks, the three context checking parameters with their thresholds, and the power gain pg_v^w of the signal between v and other vehicle w . When the network is active, vehicles will start beaconing their new styled beacons every T seconds. The clusters are formed and modified based on the received signal strength values.

Results and Discussion:

Conforming with the existing regulations of DSRC standards, we choose the up-to-date elliptic curves recommendations of 128 bit security level. The adopted beacon generation rate T is 100 msec at 6 Mbps data transmission rate. The T_{C_v} context timer value is four times the T beacon generation rate. We assume

the number of cars in v 's neighborhood to grow up to certain limits. The signal strength pg_v^i values of the received beacons by vehicle v are normalized in our simulations to probability values in the $\{0,1\}$ interval depending on the distance between the sender and the receiver. To achieve a fair evaluation of the proposal effectiveness in the targeted scenario, we develop the Drop Rate γ_v (vehicle) metric for every vehicle v . To properly derive γ_v , we make use of the above mentioned performance metrics. We first redefine and set their initial and threshold values to help fine-tuning the simulation results:

1. Tolerated Communication Overhead C_{O_v} (byte) and Number of Neighbors N_{C_v} (vehicle): our scheme alternates between three frameworks, each has different authentication format and size to secure the beacons message; PKI sends two signatures and one public key, GS sends one group signature, and IBC communicates one signature, one public key, and two alias identities. The aforementioned security payload restricts the number of vehicles N_{C_v} that can acquire the limited 46 msec wireless control channel. Figure 2 shows the maximum N_{C_v} number of individual vehicles that rendezvous on the wireless medium in the three frameworks for different data rates. Since IBC has the lowest C_{O_v} load, it accommodates more vehicles.

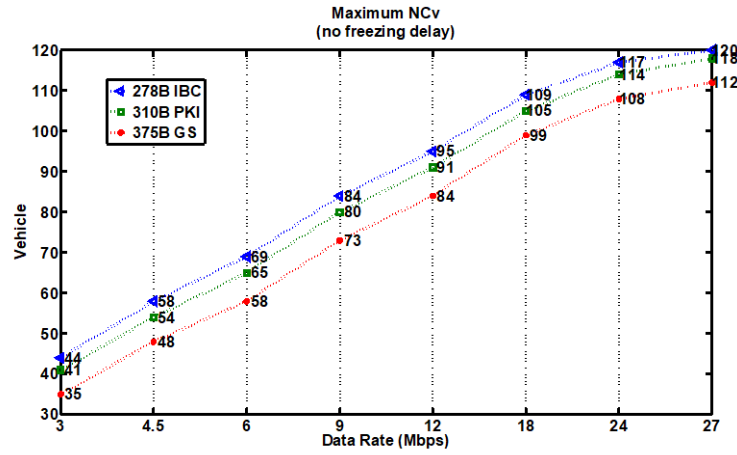


Figure 2: Maximum N_{C_v} that fits in CCH for the three authentication schemes

These maximum N_{C_v} values facilitate the choice of $\xi_{N_{C_v}}$ and $\xi_{C_{O_v}}$ thresholds. For simulation wealth, we choose $\xi_{N_{C_v}} = [mean_{N_{C_v}}, \frac{mean_{N_{C_v}}}{2}, \frac{mean_{N_{C_v}}}{4}]$ and $\xi_{C_{O_v}} = \xi_{N_{C_v}} \times average(PKI_{C_{O_v}}, IBC_{C_{O_v}}, GS_{C_{O_v}})$, where $mean_{N_{C_v}}$ is the average of N_{C_v} in each authentication framework.

2. Anonymity A_v and ξ_{A_v} Threshold: the entropy of the pg_v^i signal strength of the received beacons from vehicle i contributes to the degree of anonymity of vehicle v within the T_{C_v} context timer interval. The initial value of A_v is obtained after a single beacon interval of 100 msec. For the anonymity threshold, our simulations coin it to be $\xi_{A_v} = [4, 3, 1.4]$ when $\xi_{N_{C_v}}$ is reached.

We want to ensure that these chosen threshold values are suitable for our scenario, i.e., comparable N_{C_v} , C_{O_v} , and A_v results have to be achieved. In this sense, we compare our scheme with the three authentications for about 20 runs of T_{C_v} context timer intervals; we can easily see that in its individual case,

our scheme achieves comparable anonymity level and number of neighbors performance for all of the $\xi_{N_{Cv}}$ values. Moreover, for the overall beacon overhead C_{Ov} , our scheme introduces the same small overhead of our new IBC scheme; this makes it more effective than the other two pure authentications: PKI and GS. For example, our scheme achieves on average an overhead gain of 6%, 3.4%, and 8.76% in comparison with the pure PKI framework for the three values of $\xi_{N_{Cv}}$ threshold, respectively. Compared with GS, our scheme's overhead is 22.69%, 20.1%, and 24.9% less than GS overhead for all of the $\xi_{N_{Cv}}$ threshold choices.

Having chosen such thresholds, we are led automatically to have lower drop rate γ_v in comparison with PKI, IBC, and GS pure authentications. We define the drop rate here to be the total number of vehicles that cannot capture the wireless medium due to the limited CCH width and total communicated beacon size. Figures 3, 4, and 5 aid our claim where our scheme outperforms the other authentications for the selected threshold values, especially when $\xi_{N_{Cv}} = \frac{N_{Cv}}{4}$; for example, although the scheme's γ_v approximates the drop rates of the pure authentications for $\xi_{N_{Cv}} = mean_{N_{Cv}}$, it has an average of 43.4%, 37.8%, and 26.6% gain in comparison with IBC, PKI, and GS frameworks when $\xi_{N_{Cv}} = \frac{N_{Cv}}{2}$. For $\xi_{N_{Cv}} = \frac{N_{Cv}}{4}$, the interchange has an 80.3% gain over IBC, a 78.55% gain over PKI, and a 74.3% gain over GS framework.

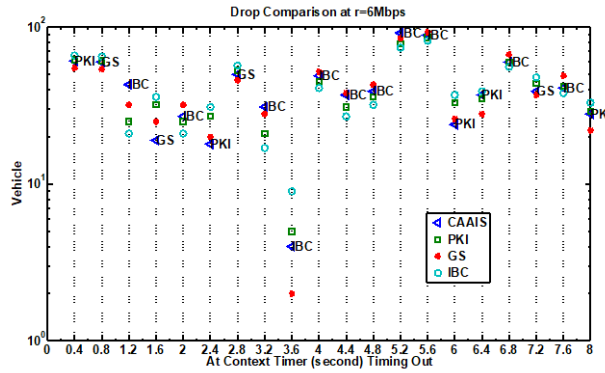


Figure 3: Drop rate comparison for $\xi_{N_{Cv}} = mean_{N_{Cv}}$

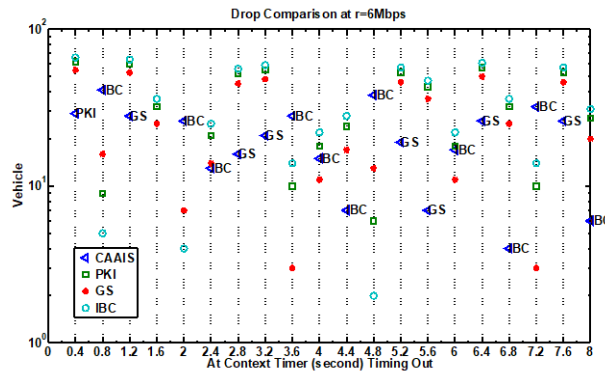


Figure 4: Drop rate comparison for $\xi_{N_{Cv}} = \frac{N_{Cv}}{2}$

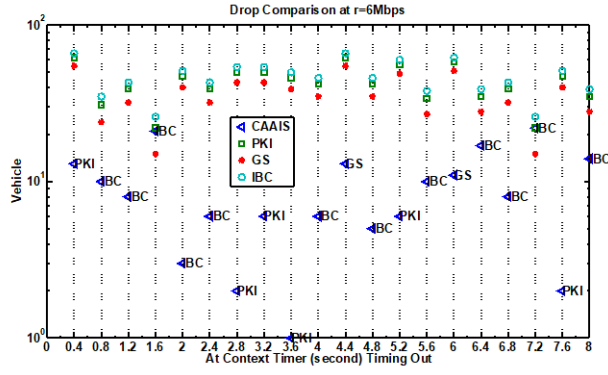


Figure 5: Drop rate comparison for $\xi_{N_{c_v}} = \frac{N_{c_v}}{4}$

The interchanged scheme achieves better performance than the case of having one pure secure authentication throughout the network lifetime; our approach is computationally fast and does not compromise the autos' anonymity. Also, the scheme achieves lower vehicle drop rate in comparison with the available pure frameworks.

Conclusions and Future Extensions

In VANETs, the number of vehicles, which can concurrently capture the wireless medium, is limited by the width of the CCH channel and by the type of the utilized authentication framework; some frameworks have less communication overhead while others have more anonymous traits; therefore, sticking to only one framework is unfair. In this sense, we introduced in this research a context-aware authentication interchange scheme that mixes three cryptographic frameworks: PKI, GS, and IBC. In our scheme, each PKI vehicle checks its surrounding every a specific time interval: if the vehicle finds that the neighborhood is crowded, the car switches to a lower overhead IBC authentication; if the surrounding is sparse, the vehicle switches to a more anonymous GS authentication. Our mingled-authentications scheme shows a better performance than the case of using single pure authentication; our scheme achieves lower vehicle drop rate in comparison with the three schemes. Our analysis does not consider the competition for CCH. It is one of the future extensions that we are deliberating on to see how such factor can affect the performance of the scheme in comparison with the pure IBC, PKI, and GS frameworks.

Cognitive Radio Based Communication
Sub-Project PI: Prof. Eylam Ekici
Dept. of ECE (OSU)

Cognitive Radio Based Communication

Major goals – The major goal of our effort is to evaluate the performance of the vehicular cognitive radio networks to cater to the needs of both sensing and communication functions of vehicular networks.

Accomplishments: During this reporting period, we investigated the performance of a joint communication and radar system in the 79GHz band, where radar and communication functions are co- located on the vehicles. The specific objective of our study was to perform a comparative analysis of resource allocation methods in the radar band so that communication can be sustained while maintaining the baseline performance of the radar system, as if the radar system were operating on its own. To that end, we took a holistic approach and assessed the performance of our developed communication protocol to enable establishment, maintenance, and control of the communication actions in the radar band with the assistance of the DSRC system. Our simulation studies have revealed the following:

1. DSRC band is necessary to serve as a control channel for successful facilitation of cooperative communication and sensing among vehicles
2. The high bandwidth made available for communication needs to be expanded to multi-hop cases, which is only possible through coordination among vehicles.

Dissemination: Two journal papers summarizing our research outcomes have been published in IEEE Vehicular Technology Magazine and IEEE Transactions on Wireless Communications.

Products:

You Han, Eylem Ekici, Haris Kremo, Onur Altintas, Throughput-Efficient Channel Allocation Algorithms in Multi-Channel Cognitive Vehicular Networks, IEEE Transactions on Wireless Communications, vol. 16, no. 2, pp. 757-770, February 2017.

You Han, Eylem Ekici, Haris Kremo, Onur Altintas, Vehicular Networking in the TV White Space Band, vol. 16, no. 2, pp. 52-59, June 2017.

Impact: Development of the principle discipline: The effort during this reporting period builds upon our previous findings that revealed that long-held beliefs about the use of 802.11p protocol as a very good, real-time communication alternative were indeed unfounded. Our new studies show that it is possible to utilize radar bands allocated for vehicular radar systems to communicate data across vehicles. The resulting increase in the available bandwidth is significant enough to warrant further investigation of practical methods to jointly utilize this channel, and also to model the radar band for the purpose of communication.

EEG and Lane Change Intent Evaluation on a Driving Simulator

Sub-Project PI: Prof. Umit Ozguner

Department of ECE
The Ohio State University

EEG and Lane Change Intent Evaluation on a Driving Simulator

I. INTRODUCTION

Driver intent estimation is an important problem area for the future of intelligent vehicles, assuming that vehicles with varying levels of autonomy as well as non- autonomous, human-controlled cars will be sharing the road in the near future. Electroencephalography or EEG is a measure of the relative voltage at different locations on a person’s scalp, which corresponds to brain activity and has been used in the medical field for many years. While EEG may not be a practical sensor to force on all drivers, it does give us some insight into the way humans make their driving decisions. The lane change scenario was chosen as a simple but important example of a routine driver decision whose outcome might be difficult for an observing vehicle to predict based on vehicle dynamics alone.

A. Problem Formulation

We would like to answer the question, *can we use a low-cost, wireless EEG collection device as a sensor to indicate a driver’s intent to make a lane change in a simulated driving environment? If so, how?*

B. Related Work

Putting an EEG sensor on a driver in a driving simulator is not a completely new idea. The authors of [1] examined alpha waves in the EEG spectra of subjects playing “Need for Speed” and determined that the subjects are less attentive upon replay of a simulation. Driver fatigue and drowsiness studies have been perhaps the most popular and successful use for EEG in a driving simulator. An example of a drowsy driver study is found in [2], where the measure of drowsiness from the EEG is validated with the driver’s actual performance, measured by his deviation from the center of the lane. Another common thing to study with EEG and driving simulators is the effect of brain abnormalities on driving, such as the tests done with epileptic patients in [3]. To our knowledge, no-one has attempted to use EEG to predict the onset of non-emergency driving maneuvers such as a lane change to pass a slow-moving car.

II. METHODS

In an attempt to answer the question above, a set of experiments were devised using a driving simulator and an EEG measurement device to be worn by the driver.

A. Experimental Equipment

1) *Driving Simulator*: The driving simulator used for experiments is a tabletop version developed by Real Time Technologies. The simulator setup is shown in Figure 1.



Fig. 1. Driving simulator from Real Time Technologies

2) *Emotiv EEG Device*: EEG collection devices used in medicine are very costly and usually inconvenient to use, but recently several companies have released low-cost, wireless versions with the sensors pre-mounted on a headset. Marketing for such devices has typically been geared toward gaming (using the EEG as a brain-computer interface), but research editions with access to the raw EEG data are also offered. We chose the Emotiv brand EEG device, shown in Figure 2, and a review of which is given in [4]. The device features 14 EEG channels based on the traditional 10-20 sensor location scheme as well as a gyroscope to measure head motion.

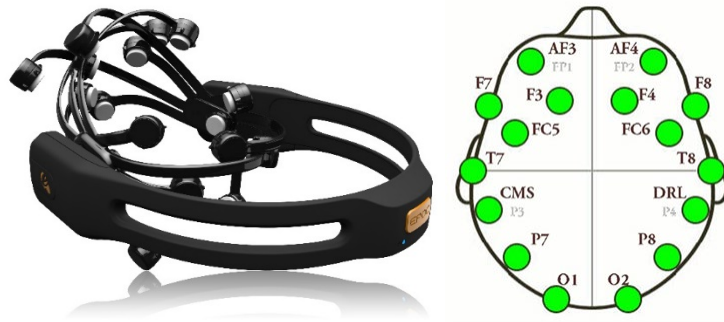


Fig. 2. Emotiv EEG Device (image courtesy of Emotiv)

Experimental Setup

An experiment was devised in which a volunteer driver would wear the EEG device while completing a series of lane change maneuvers. The simulator scenario chosen was a four lane highway with a variable amount of ambient traffic other than the car or cars to be passed in the lane change maneuver. In all runs, the subject vehicle begins in the right lane and is asked to drive as realistically as possible, keeping a speed of about 60 mph. In the first run, a slow-moving small car begins 300 m in front of the subject's starting point in the right lane, and is eventually overtaken and passed by the subject. That car becomes a large truck in the second run, and, in the third run, a tightly spaced convoy of two cars. Initially, one subject completed the three runs three times each with the amount of ambient traffic set to zero. The time-synchronization between the two computers that run the two pieces of hardware was an issue. A manual system time reset was executed immediately before the experiment and system time-derived time stamps were applied to all data streams. This process allowed the data to be synchronized to less than a second.

B. Experimental Results

Figures 3 through 7 show the EEG data from the tests with just one car to pass alongside the y-position data of the subject vehicle (the lane change) plotted on the same time axis. There are five plots because the EEG device has 14 channels plus two gyros, all of which are plotted between those five figures. Immediately noticeable are a series of interesting “blips” in many of the EEG channels (see channels F7, F3, FC5, T7, P7, FC6, P8, and F8) that come right before the lane change maneuver begins. Figure 8 shows the positions of the electrodes mounted on the Emotiv EEG headset. It is possible that this blip pattern could indicate the driver's intent to make a lane change, but I hypothesized that the high amplitude spikes could be artifacts related to eye movement, that is, when the driver looks at his mirrors to see whether a lane change is safe. They could not correspond only to blinking (another typical artifact in EEG readings), since the subject would have blinked many times in 40 seconds. This hypothesis is consistent with the sorts of examples given in EEG technician manuals I have read such as [5]. Since the eyeball acts as a slight electric dipole, its rotation along either axis will impact the electric field around the head, which will show up in the EEG record. Vertical eye rotation causes field changes along the sagittal axis, while horizontal eye rotations cause field changes along the coronal axis, according to [6]. Many papers relating to signal processing and EEG focus on eliminating artifacts which appear due to eye blinks and eye movement, so their presence is well documented.

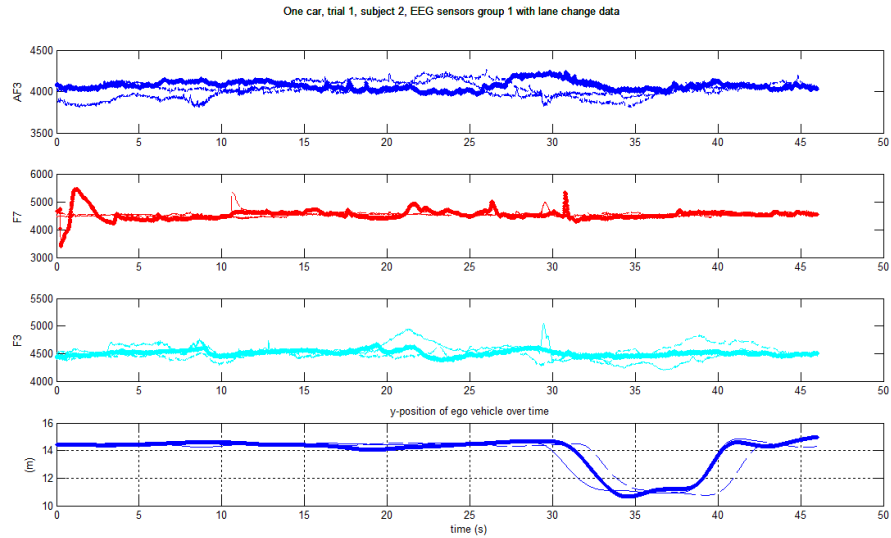


Fig. 3. First group of EEG data channels for the one car pass case. The y-position of the subject vehicle is shown at the bottom along the same time axis. Three trials with the same subject and scenario are shown by the three line types. Note the “blips” in the EEG right around the time that the passing maneuver begins.

To test this hypothesis, the experiment was re-done, this time with the subject instructed not to look at his mirrors at all, but to keep his eyes straight ahead on the road.

Trials with the same subject and scenario are shown by the three line types.

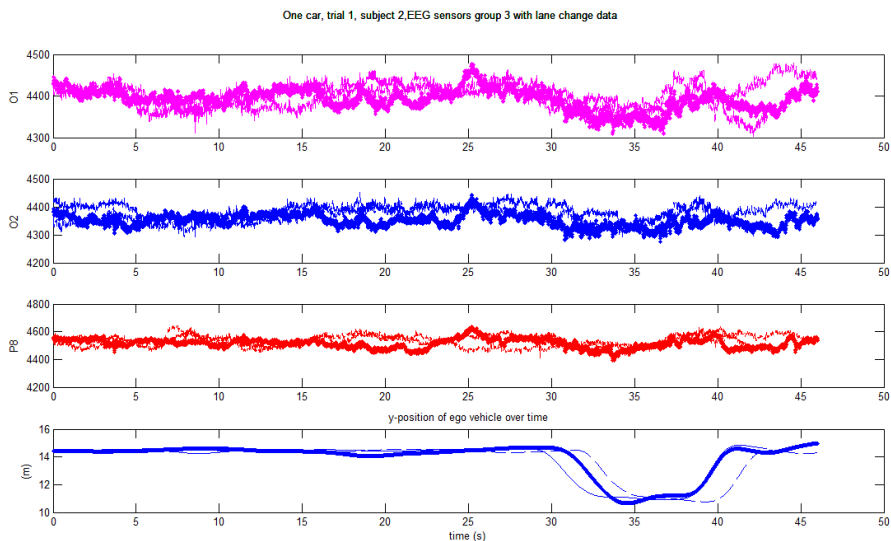


Fig. 4. Emotiv EEG channel positions; based on traditional 10-20 system (image courtesy of Emotiv) spectrogram for a sample channel (characteristic of the other channels) from each case, the normal driving case and the looking straight ahead only case, is shown in figures below. In the normal driving case, high frequency content is

present around the time that the lane change starts, while the same part of the straight-looking case is flat.

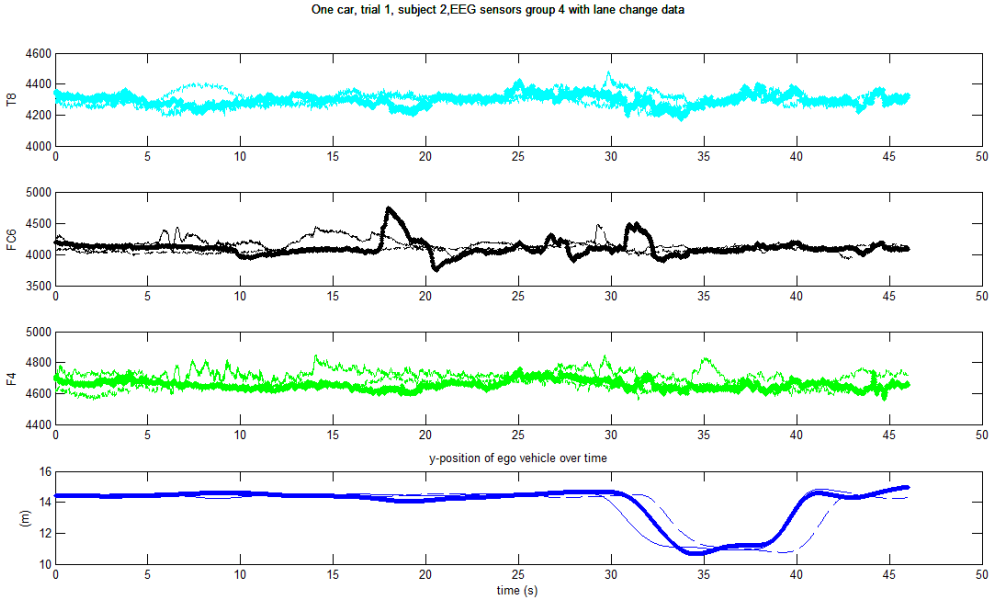


Fig. 5. First group of EEG data channels for the one car pass case when the subject is instructed to look *straight ahead*. The y-position of the subject vehicle is shown at the bottom along the same time axis. Note that the “blips” that seemed interesting in Figure 3 are not apparent here.

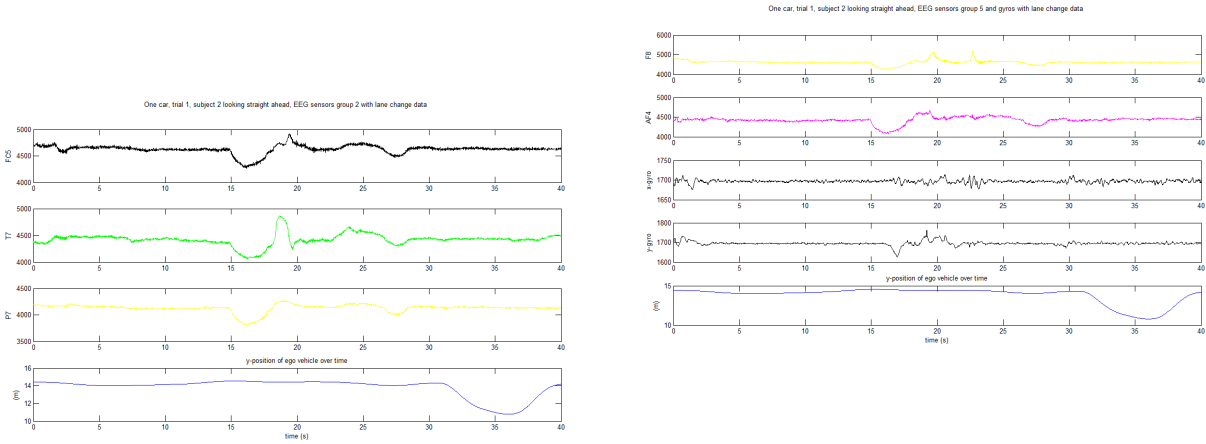
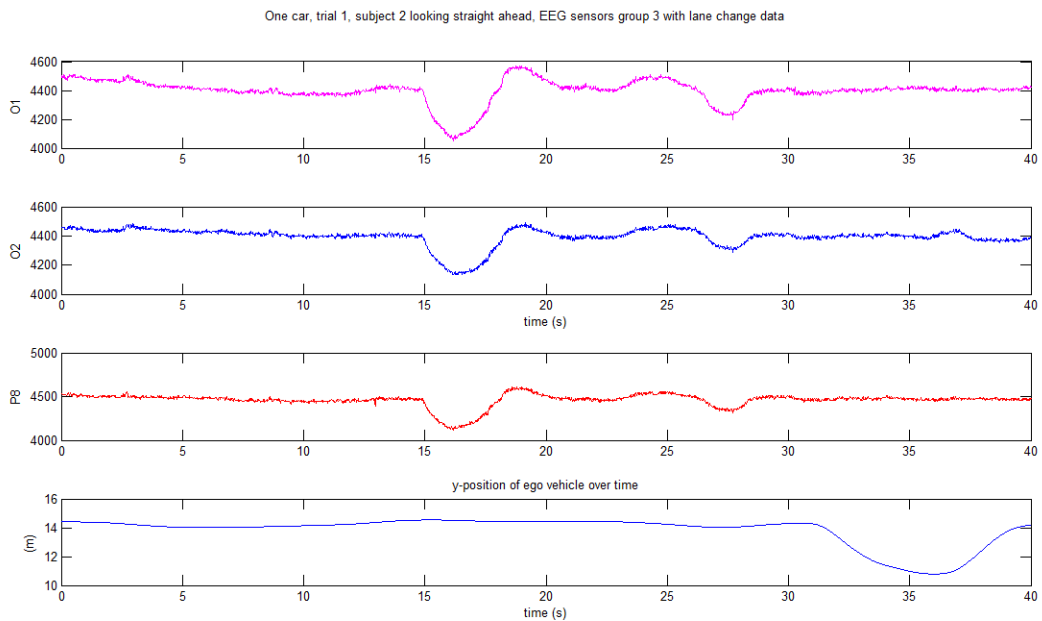


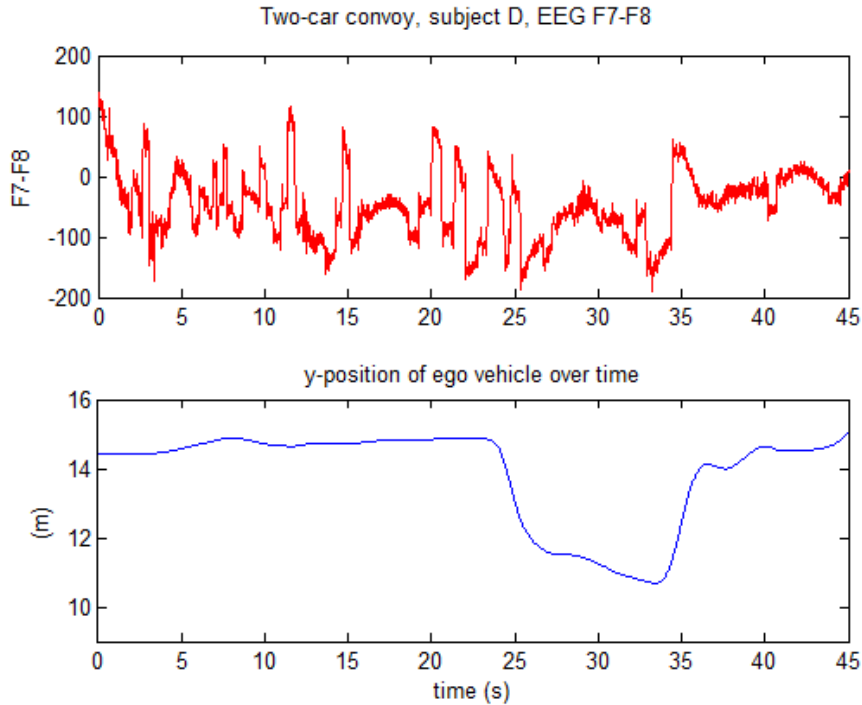
Fig. 6. Fourth group of EEG data channels for the one car pass case when the subject is instructed to look *straight ahead*. The y-position of the subject vehicle is shown at the bottom along the same time axis.

In order to get a better look at eye movement and to possibly separate out the side-to-side eye rotations from the up-and-down rotations, some signals were combined. Side-to-side eye rotation should produce high amplitude artifacts in this trace, as seen when the driver presumably checks his mirrors right before he makes the first lane change in all three trials. Note that one of the eye movements is in the opposite direction to the other two, which would suggest that the driver did not always rely on the same mirror when making his lane change. Also note that similar shapes and patterns are found elsewhere in the record, though the greatest concentration does appear to be right before the lane change. It is of course sensible that a conscientious driver would check his mirrors or glance around him at times other than right before he intends to change lanes, but Subject 1 knew that there were no cars on the road other than the one he was passing.



In order to see the up-down eye movements, one must compare the voltages from a pair of electrodes that spans the eyeball on the vertical axis. However, none of the Emotiv electrode pairs have quite that orientation. Therefore, there is no corresponding eye-movement plot for vertical eye movements using this sensor. I did try to get close by subtracting some of the channels that are nearly vertical from each other and near the eyes, but there was no meaningful pattern that could be seen. This conclusion is supported by the fact that the Emotiv development software includes an eye gaze detection program, but it only measures sideways eye motion. Theoretically, with a different electrode setup, vertical eye gaze would be possible to detect in the same way as horizontal eye gaze.

From data collection of subject D (with extra ambient traffic, natural driving, one car to pass), the subtraction of T7 from T8. High amplitude fluctuations in this trace should correspond to side-to-side eye movement.



III. DISCUSSION AND CONCLUSIONS

Success in this project could mean one of two things. First, we could find out that the EEG signals from the low-cost sensor do indeed give a clear indication of a driver’s intention to make a lane change or pass a car. This indication may be predicated on a certain driver behavior that not all drivers exhibit, such as checking a certain one of his mirrors. Second, we could conclude that there is no consistent indication of a driver’s resolve to begin a lane change or that the indications that exist are not unique enough to be useful for this task.

Traditional studies done with EEG have found success in ascertaining a driver’s mental state such as mood, drowsiness, alertness, stress, or emergency reaction. These indications are usually valid over a longer, fuzzier time interval than the interval of a few seconds or milliseconds right before a new routine driving maneuver. They are also usually found using a medical-grade EEG device with many more sensors and lower noise. At present, it appears that the clearest indication of a lane change from the raw Emotiv EEG time and frequency data comes from eye movement. Assuming that a driver routinely checks his mirrors before performing a lane change or passing maneuver, this information could be enough to identify the fact that a driver is making a lane change. However, because of the nature of the eye movement artifacts in the EEG, this information would not precede the actual action of checking the mirrors, since it is the actual eyeball rotation that changes the electric field around the head, and not the premeditated intention to do something new. There are other less invasive and more practical ways to detect eye movement,

which suggests that EEG is probably not the best sensor for the job of online detecting a driver's intent to make a lane change.

However, it is feasible that a pattern classification procedure such as that found in [7] could be used with a series of EEG training data to identify a subject's typical eye movement patterns and habits. This knowledge could be useful in characterizing types of drivers. The eye gaze information could be combined with other existing EEG capability such as detecting the driver's mood and alertness. For example, if a driver routinely checks his mirrors before a lane change and also maintains a healthy level of alertness, the driver is probably more trustworthy than another driver who neglects to check his mirrors or tends to be distracted. The general driving habits and level of consistency identified by this process could be useful in adjusting individual decision probabilities for driver state estimation routines such as those found in [8], assuming that the identity of the driver and his characteristics are known by an intelligent vehicle online. In this way, driver analysis with EEG could be useful to autonomous vehicles and active safety systems without the need for human drivers to be constantly wearing EEG devices in their cars.

REFERENCES

- [1] M. A. Schier, "Changes in eeg alpha power during simulated driving: a demonstration," *International Journal of Psychophysiology*, vol. 37, no. 2, pp. 155–162, 2000.
- [2] C.-T. Lin, R.-C. Wu, T.-P. Jung, S.-F. Liang, and T.-Y. Huang, "Estimating driving performance based on eeg spectrum analysis," *EURASIP Journal on Advances in Signal Processing*, vol. 2005, no. 19, pp. 3165–3174, 2005.
- [3] D. Kasteleijn-Nolst Trenité, J. Riemersma, C. Binnie, A. Smit, and H. Meinardi, "The influence of subclinical epileptiform EEG discharges on driving behavior," *Electroencephalography and clinical neurophysiology*, vol. 67, no. 2, pp. 167–170, 1987.
- [4] K. Stytsenko, E. Jablonskis, and C. Prahm, "Evaluation of consumer EEG device emotiv epoc," in *MEi: CogSci Conference 2011, Ljubljana*, 2011.
- [5] F. M. Dyro, *The EEG Handbook*. Frances M. Dyro, 1989.
- [6] G. Gratton, "Dealing with artifacts: The eeg contamination of the event-related brain potential," *Behavior Research Methods, Instruments, & Computers*, vol. 30, no. 1, pp. 44–53, 1998.
- [7] S. Haufe, M. S. Treder, M. F. Gugler, M. Sagebaum, G. Curio, and B. Blankertz, "EEG potentials predict upcoming emergency brakings during simulated driving," *Journal of neural engineering*, vol. 8, no. 5, p. 056001, 2011.
- [8] A. Kurt, *Hybrid-State System Modelling for Control, Estimation and Prediction in Vehicular Autonomy (Dissertation)*, 2012.

Analyzing and Mining Big Data of Driving Videos for Crash Avoidance

Jiang Yu Zheng* (jzheng@iupui.edu)

Mehmet Kilicarslan (mkilicar@indiana.edu)

Addresses:

1. Department of Computer Science
Indiana University Purdue University Indianapolis,
Indianapolis, IN, 46202
2. Transportation of Active Safety Institute
Indiana University Purdue University Indianapolis,
Indianapolis, IN, 46202

ABSTRACT

Purpose: the purpose of this project is to construct an online video database to host big data of naturalistic driving video including crash and near miss cases from recent populated vehicle borne cameras for accident verification and the crash avoidance technology development. A series of new video processing methods is developed for large-scale driving video indexing, browsing, visualization, automatic event detection, and accurate measuring of vehicle and environmental parameters in the videos. Big Data mining is applied to summarizing parameter distributions for extracting critical factors of crash in the video dataset. The video and data have been uploaded for analyzing accidents and surveying results for the design of vehicle safety functions and crash testing scenarios.

Methods:

Building an online database to collect driving video on a cloud computing platform like YouTube for research uses, and creating its data-reduction format called temporal profile for browsing driving history and measuring parameters of vehicle and road environments. The data can provide ground truth for vision sensor development and algorithm testing, crash accident analysis and survey.

Automatic extraction of vehicle motion and environment related signature events from driving video and associated GPS output, and index video clips with tags. The signature events may include dynamic actions of vehicles such as near miss, potential collision time, ego-motion and maneuver actions, and interactions with other vehicles, pedestrians and bicyclists, as well as environmental attributes such as road width, illumination, traffic flow, etc.

Mining information in the signature events extracted from large volumes of driving data. As an example, we mine the road appearance under various weather and illumination conditions from a large set of video. This provides the detectability of road edges, which is beneficial to the system development to prevent road departure. We have used K-mean unsupervised learning method to cluster the weather and illumination patterns on road and off-road for identify road edges in safety and autonomous driving.

Results: The results have been published in the IEEE ITS Society Conferences in details. Online video database has been constructed for retrieval, and basic functions to analyze video with profiles are developed. Several data mining and video sensing methods have been studied to estimate potential collisions with vehicles and pedestrians when vehicles are moving on road.

Conclusions: This work tackles the problem of processing and mining driving videos from naturalistic driving. Architecture to store driving video on a Cloud has been built to collect a large-scale video database. Tagging and retrieval of these video data are possible online through web access. In order to handle the huge data size of video, we extract the compact representation of driving video called temporal profiles that includes motion profile and road profile. This reduced the data by one dimension to $1/360^{\text{th}}$ of the video in size. By extracting the signature features in such spatial-temporal images, we can investigate road environments, vehicle interaction, as well as the driving behavior of drivers. Particularly, computing the TTC, and pedestrian detection in the motion profiles directly serves collision avoidance of vehicles on road. Our investigation of road appearances under various weather and illumination conditions

further helps the prevention of road departure and improvement of road infrastructure.

1. INTRODUCTION

Vehicle borne cameras have become feasible and popular in recent years and many manufactures will equip their vehicles with front cameras in future years. In addition to recording accident moments and providing panoramic views to assist parking, videos taken in normal driving are also archived to improve driving experiences for accident avoidance. Driving video has been increasingly uploaded to cloud media websites via mobile communication but their analysis has not been tackled. It is truly Big Data including large sections of normal driving, frequent near miss, and rare accident cases in datasets. A cloud computing platform is required for data mining in driving video.

The driving video contains huge amount of information related to driver's behavior, interaction with surrounding vehicles and pedestrians, and road infrastructure and environment. Mining these data to extract meaningful statistical information is very challenging and beneficial to vehicle safety design, crash avoidance, and traffic infrastructure improvement. For example, knowing the distance distribution between vehicles helps the design of vehicle-to-vehicle wireless network for safety communication between vehicles.

Big video data in such a large scale are almost impossible to examine manually. Searching functions for accident and near miss clips as well as environmental information on road have to be developed to reach the clips of interest. Automatic video analysis algorithms, named contents based retrieval, are demanded to scan terabytes of video database for target clips. For the accident clips, measuring tools for various parameters at those moments are demanded for analyzing the causes and influences from surroundings.

2. METHODS

2.1 Online Driving Video Database

2.1.1 Online Database Construction

We first construct database to host terabytes of driving video clips and their indexes. The online database is named Drivingtube hosted in the School of Science by Computer Science Staff, managed by the student database group in our team. The database is a relational database built on

SQL server for retrieval and is supported by PHP program made for online access via internet. Figure 1 shows the front page of the database website and the web address of the database is at drivingtube.cs.iupui.edu.

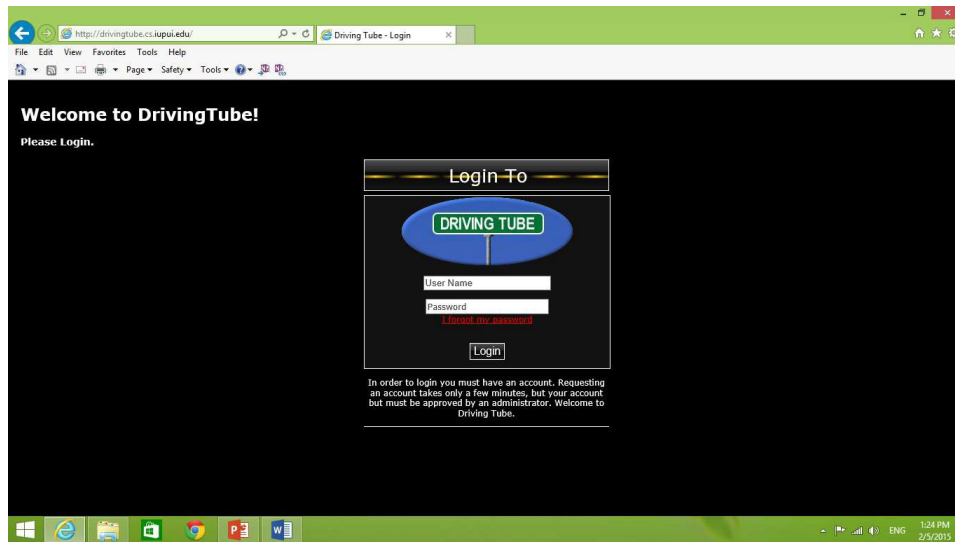


Fig. 1: Online database Drivingtube hosting driving videos from vehicle borne cameras.

The Drivingtube database has the following functions constructed as follows:

- Video Clip Retrieval Based on Attributes

Each video is tagged with attributes such as “turn right”, “cloud day”, “children”, etc. Through the panel of query, users can select attributes (key words or tags) to submit a query as shown Fig. 2. The search message is sent to database server by PHP program. The SQL language searches the database to select video clips with their attributes matched to the query. The video clips are displayed in a gallery page, which can be flipped page by page according to the total number of video clips satisfying the query specification. The video search can use a composite query by defining multiple attribute values. The total number of the video set that satisfies the query is also displayed. The attributes are currently adopted from the scenario design of TOYOTA 110 Car Naturalist Driving Data [4].

To access each video clip, a separate window is pop off after the video icon is clicked in the gallery page. In a video clip page, the video in MPEG format is played by QuickTime codec (Fig. 3). A motion profile of the video clip contains orientation (horizontal axis) and time information (vertical axis) of surrounding scenes is also displayed as a spatial-temporal image.

The attributes of the video clip currently tagged by users are further displayed below the motion profile.

The screenshot shows a web browser window with the URL http://drivingtube.cs.iupui.edu/video_gallery.php. The page features a navigation bar with a "DRIVING TUBE" logo and menu items: Video Gallery, Users, Tags, Help, and Admin Panel. On the left, there are sections for "Categories" (Logoff, Adults, Children, Urban, Rural) and a "Search" form with various filters like Condition, Driving Direction, and Light Condition. The main content area is titled "Videos" and displays a grid of 12 video thumbnails, each labeled with a number from #0 to #11. Navigation links for "Previous", "Beginning", and "Next" are visible above and below the grid. At the bottom, it states "Driving Tube is a Production of Computer Science © 2014 IUPUEDEU".

Fig. 2 A gallery page displaying the video clips in the database searched with query.

<http://drivingtube.cs.iupui.edu/video.php?vid=002995>

[Video Gallery](#)
[Users](#)
[Tags](#)
[Help](#)
[Admin Panel](#)



Categories

- > Logoff
- > Adults
- > Children
- > Urban
- > Rural

Search

Children:
 Adults:
 Condition:
 Driving Direction:
 Driving Environment:
 Lane Turning From:
 Lane Turning Into:
 Light Condition:
 Vehicle Position:
 Vehicle Direction:
 Roadway Alignment:

#23

[Download](#)
 Action:
 Contains Abnormal Pattern: 0
 Date Entered: 2014-04-11 13:21:15
 Last Modified: 2014-04-11 13:21:15
 Deleted: 0
 Condition: clear
 Driving Direction:
 Driving Environment: urban
 Frame Number: 71
 Video ID : 00299539-5b8a-4c39-b343-6929e44ac288
 Lane Turning From: 0
 Lane Turning Into: 0
 Light Condition: other
 Next Frame: 0
 Number Of Adults: 3
 Number Of Children: 0
 Pattern Tag: NaN
 Vehical Position: center of lane
 Potential Conflict: 0
 Previous Frame: 0
 Roadway Allignment: straight
 Road Component: other
 Road Type: other
 Total Lanes After Turning: 0
 Total Lanes From: 0
 Traffic Control:
 User ID: 1213
 Vehical Direction: straight
 Version: behavior_analysis_revised_v12
 Video Name: 0448101112132300063.MOV_5050_H1062.mp4
 Video Num: 23

Fig. 3 Individual video page with the video clip, motion profile, and attributes.

□ Uploading Video Clips

We have succeeded in individual video clip uploading through the menu of the website. The video can be AVI and MPEG format. We are working on a better interface to allow users to select tags or attributes of the uploaded video. Key frames will be extracted from the video for webpage display.

To facilitate understanding of dynamic events in driving and accident, a motion profile is extracted at the time the video is uploaded. We have succeeded the motion profile generation on PC and now we have built this function as SERVER SIDE PROGRAM so that it can response to user uploading online. The users will have to select the position of horizon by mouse in the webpage because the video may be captured with various camera tilt in-car. Our program then extract the motion profile around the selected height.

- Downloading Video Clips

Through each video page, the video can be downloaded in AVI format. This is done in online version to help researchers to analyze a video of interest. At the same time, we have realize offline batch downloading of video sets. A video list can be created through database query and their disc locations are further provided as a file online. Due to the large data size of video dataset, the downloading is performed offline in the lab.

- Administrator's Page

In addition to above functions, we are also working on administrative pages to manage the uploaded video data and organize, extend, and maintain the database for robust use in the future.

2.1.2 Motion Profile of Video for Event Visualization

As video clip gets long in time, it is not easy to grasp the information of entire video globally because of the sequential access mode of video. To facilitate video browsing by ITS experts, we have developed a new image scheme called temporal profile of video, in which the motion profile accumulates video data near the horizon in the forward camera and the road profile scans the road surface as a road map. We pile all the data from consecutive frames to an image as shown in Fig. 4. All the vehicles move on the ground, pedestrians and bicyclists will be captured at least partially by the data sampling belt around the horizon in every video frame. The

continuous motion of background and other vehicles are shown as trajectories in the motion profile image as shown in Fig. 4b. Along with the video clip, the entire motions caused by the vehicle ego-motion and other vehicles are displayed in a time precise manner for users to identify the position and moment of vehicle action and surrounding events.

y



x

(a)

t



x

(b)

Fig. 4 A frame (top) of urban driving video and the motion profile (bottom) vertically condensed from the red rectangle in frames. The motion profile shows the right turning vehicle (white) in front with turning light blinking, passing vehicles in large curved traces on left side, and pedestrians' walking trajectories as chains. Time of each event is recorded accurately along the vertical time axis in the motion profile.

The motion profile is generated when the video clip is uploaded by users. Users have to specify the horizon height in the video frame after a key frame is provided from the database server after

the video uploading is finished. Because the cameras are set in vehicles with various orientations, the horizon cannot be detected robustly by an algorithm. We thus choose the manual specification of the horizon by users on webpage.

2.1.3 Road Profile for Environment Survey

From a video clip, a road profile is also generated as well to record scenes along the street and road surface (Fig. 5). They will help manual searching and browsing of large video sequences. It allows for researchers in ITS area to identify the clips of interest based on passed road scenes and measure the time and actions in the driving history. The road profile has one axis as time or route direction, and the other axis as the orientation ranging from left side scene, road forward, and right side scene. The road profile is sampled from a U-type curve between the horizon and vehicle hood in the video to cover road surface and side scenes. Environment information, for example, road roughness, wetness, brightness, etc. and driving actions such as lane change, turning, and vehicle passing can be observed in the road profile. The road profile is suitable for long video clips. We are currently using it in data analysis and mining of long distance driving.



Fig. 5 A road profile scanned from a curve in the video frames overtime to record driving scenes along an urban street. The sampling curve in the video frame passes ground and two sides to scans scenes and road as the vehicle moves forward. The horizontal axis is the time and the vertical axis is the orientation in the camera field of view.

As a simplified version, the road profile can also be captured only on road surface and off-road materials. As shown in Fig. 6, a sampling line is set at a fixed height below the horizon in the video frame to sample the distance about 15m ahead of vehicle/camera. The on road and off-road appearance collected from big-data of video will reveal the possibility to detect road edges to guide the vehicle in addition to the lane mark detection equipped on many vehicle already.

Figure 7 displays the road profiles for 5 min driving under various weather and illumination conditions.



Figure 6 Four sampling regions in video frame for weather clustering.

The database is being tested internally within research groups. Access control is applied at several levels for public users, research groups, and database administrators. This will become a cloud computing infrastructure for online crash-survey. The processed data are accessible to uploading users. We also select some sample video set with ground truth from the database as benchmarks with privacy factors removed for vision and sensor researchers and developers to test their designed algorithms on accuracy and performance.

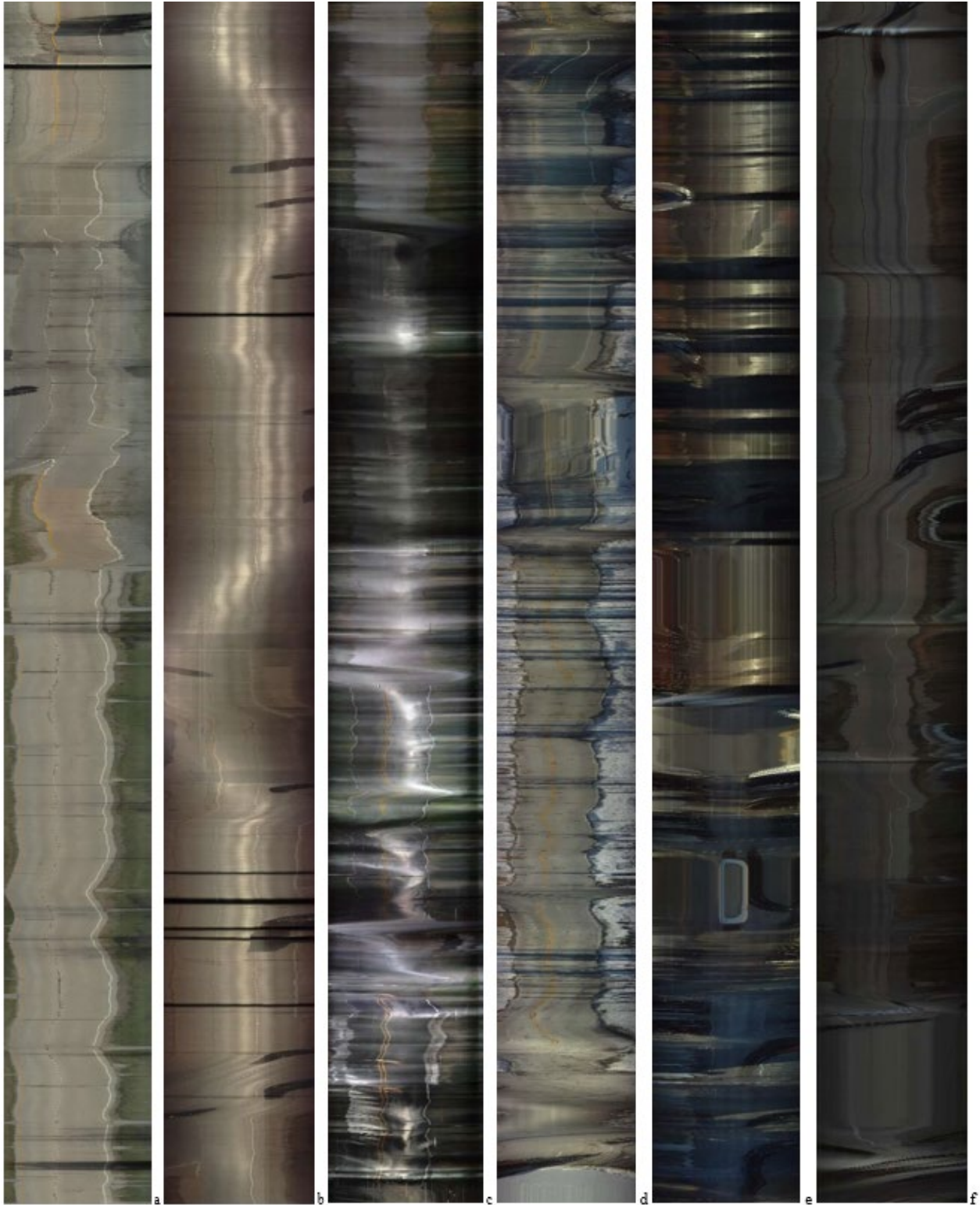


Figure 7 Road profiles captured different weather and illuminations. The time axis is upward. (a) Sunny back to the sun, (b) Sunny facing the sun with highlight on road, (c) Rainy on wet road with specular reflection of sky. Specular reflection is more dominant than road edges. (d) snow-covered

road with partial shadow, (e) heavy shadow on urban road with road partly visible, and (f) raining day. Road edge is barely visible.

2.2 Automatic Event Detection and Tagging in Video

For the survey of various information, automatic analysis of thousands of video clips by computer vision is indispensable; manual tagging is laborious and it contains bias and errors hard to evaluate. To prepare more advanced functions than a simple video database, our automatic signature event detection from video can result in three categories: (a) Interactions with walking pedestrians, bicyclists, and other vehicles with their speeds, distances, potential collision time, and count numbers both in stopping and driving periods; (b) Environments including road width, road roughness, illumination in night, weather influences, signal and vehicle light timing, traffic flow around, parking space, and passing areas such as residential area, shopping lot, highway, etc. (c) Vehicle ego-motion such as stop and move, pass, changing lane, and turn for knowing driver's response to the dynamic environments. Although partial data can be obtained from GPS and inertial sensor, a synchronization is necessary to cancel the delay in data output based on our current experiments. Many of these items can be obtained by examining road profile and motion profile from videos manually. We are working on several specific tasks in the following by analyzing the video data in the large data set. Automatic detection methods and algorithms are designed and tested off-line for the future online database mining. We combine computer vision and machine learning approaches in the event detection modules in the following.

2.2.1 Understanding Interaction of Vehicles with Surroundings

(a) Pedestrian Detection in Driving Video

Pedestrian detection is an important function of using video in the safety driving. The detection methods so far are mainly based on human shape recognition in the video frames. The computation cost of the complex algorithms is high and a recognition algorithm has to rely on a large sample set training or learning. Such methods have weakness in scanning large video dataset and cannot receive high accuracy in pedestrian classification and identification under various weather conditions and poor illumination. In addition to the pedestrian detection from

shapes [4], we have worked on new pedestrian detection method focusing on repetitive human leg motion, which is uniformed for all pedestrians regardless of background, clothes people wear, shape of pedestrian, etc. We look at non-smooth motion of limbs and body, i.e., the motion changes the direction at the end of a stroke or action, in the periodic walking sequence. This type of non-smooth motion is shown in the motion profile as a chain trajectory formed by “leg crossings” shown in Fig. 8.

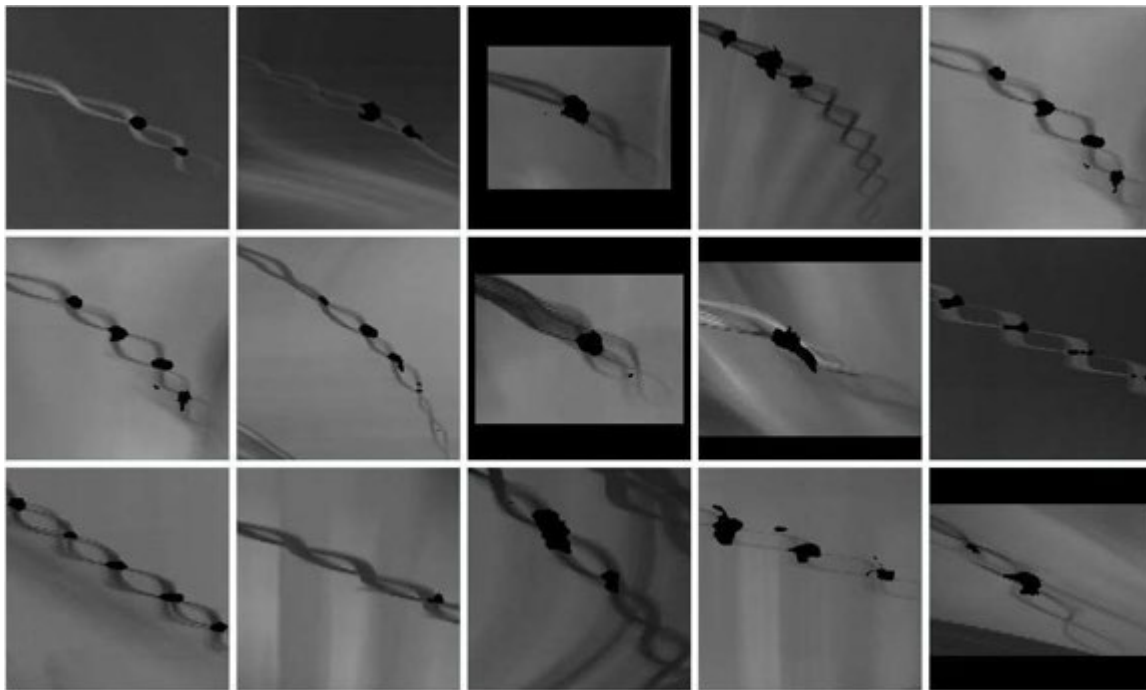
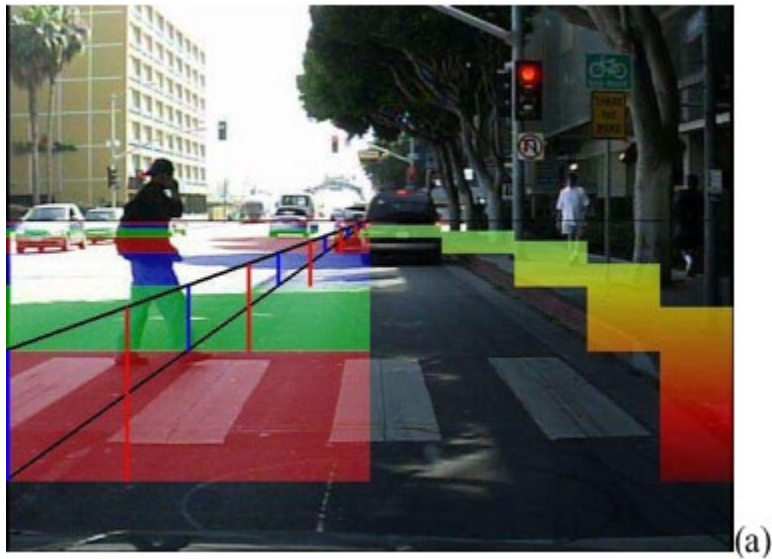


Fig. 8 Chain detection at leg crossing (marked in black) in the motion profiles indicates walking people on road. HOG features are combined with template matching of gradients in the detection. (a) Several zones from close to far are set in video space to capture the motion profiles from lower to upper image belts. (b) Pedestrian walking trajectories are detected at leg-crossings in separating with trajectories of other objects.

Because a four-wheeled vehicle has its motion along a smooth curve on the road from its mechanical design, all static background and moving vehicles thus have smooth traces in the motion profile captured by a vehicle borne camera. Only walking people generate chain trajectories from stepping legs in the motion profile, which have less confusion with background and other vehicles in the pedestrian detection. Algorithms detecting rings on the chains are investigated for achieving a high pedestrian recognition rate. A set of HOG operators is used to describe the twisted shapes of such rings at leg-crossings in the motion profile. The preliminary results have been published in IEEE ITSC14 [10, 12]. We are further test our algorithms to extend leg crossing detection to non-smooth motion detection in order to cope with more pedestrians at far distance and in crowds. The detected pedestrian with their motion traces will be used in analyzing pedestrian behavior when the vehicle is approaching.

(b) TTC and TTP Computing from Motion Profile

With the motion information in the driving video, Time-to-pass (TTP) and Time-to-collision (TTC) can be estimated from the image speed and object size in principle for entire field of view regardless of vehicles, background, pedestrians, etc. The motion profile provides trajectories of objects that can be tracked at high contrast edges in the profile image. The zero flow of trajectories indicate a possible collision. The convergence and divergence of object trajectories shows its distance change.

To compute these parameters instantly from video, we have to separate objects first in the motion profile. The occlusion of objects causes intersection of trajectories. For surrounding vehicle detection, we use a probability based model describing dangerous distances and moving directions. It can infer the target motion in the video. After the motion estimation in the video, the scenes will be classified into (a) background, (b) passed vehicles without danger, (c) passing vehicles requiring attention, and (d) dangerous vehicles with potential collision according to the position and velocity of a target trajectory tracked in the motion profile. We have developed algorithms to sort the object trajectories and compute TTP and TTC from the motion trajectories. Then, we apply it to motion profiles so that users can see the dangerous degree at any moment in the video. The potential crashing vehicles and pedestrians are extracted at every moment when

they show the motion approaching the camera, which leaves zero image flow horizontally in the frames as well as in the motion profile. Otherwise, a target is normal passing. Then TTC is estimated at the moment with potential collision based on the enlargement of target size. The action time and image velocity of a detected event are measured accurately in the temporal resolution of 60Hz, which is much finer than the output of GPS (1~2Hz) and inertial sensor (10Hz). Figure 9 shows the extraction of image velocity on the motion profile and Figure 10 shows video display with marked degree of danger from TTC. This work has been published in the conferences such as ICPR2016 [11] and IEEE IV2017 [14].

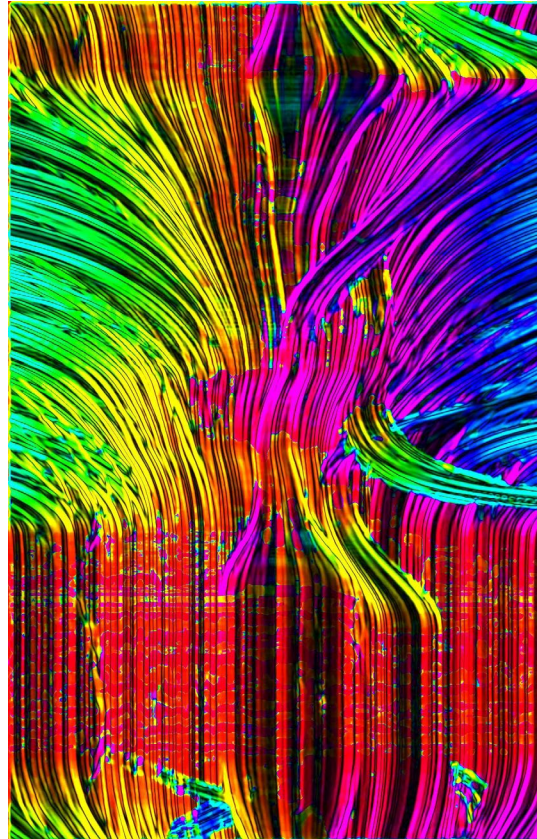


Figure 9 Motion profile marked image velocity in color computed from the tangent of motion trajectories. Red color indicates the zero-flow, while green and blue show the motion directions to two outsides.



Figure 10 A live display of dangerous degree in TTC on video frames that covers all direction in front of vehicle.

2.2.2 Environment Measuring for Automatic System Development

(a) Night Illumination on Road

One of the topics we are exploring is to measure the night illumination of road from video database. The intensity reflected from the road surface is critical for guiding driving within the road regions. The average brightness of road surface under the illumination and vehicle head light is required to measure for vehicle design and testing scenario generation.

Another testing we have started is to find the roughness of road surface including finding potholes on road. An automatic detection algorithm is designed to find road damage, uneven road area, flood area, and snow area on road in the video clips. This learned parameters will be applied to real system on cellphone for collecting road status during naturalist driving and reporting to road services.

(b) Road Edge Appearance under Various Illumination Conditions

Road side identification is important to prevent road departure and roll over, which is found to be one of the most frequently happened vehicle accidents. We start to explore the method to

separate road area and off road region in the road profile by algorithms. The clues used are color difference between the road surface and off road texture. A large set of roads should be sampled to identify the distribution of two classes of regions. The parameters to separate two classes of regions are obtained from statistics of machine learning. This work uses the road profile to achieve this goal. We have generated 6500 road profiles from 5-min driving video clips as shown in Figure 7.

We particularly focus on the visual appearances of road edges including on-road and off-road combinations under various weather and illuminations as summarized in Table 1. This provides evidence to the road edge detection algorithms and programs. It answers questions on whether road edges are visible in all situations of weathers, and what the best features for road edge detection are.

Table I: The classified weather and illumination conditions a vehicle may encounter on road. The numbers in the first column indicates the video clips of 5-min for experiments

W & I	Qualitative description of appearance
1. Sunny back to sun (93)	Including the sun at side and back direction, less shadow, rich color
2. Cloudy (83)	Including overcast and partly cloudy
3. Sunny face sun (21)	Sun in the forward direction, may have specular reflection on asphalt road surface, large shadow areas on roadside objects
4. Shadow (26)	Shadow on road surface casted from trees, etc.
5. Dark lit (43)	At dusk or sun set, sky is still bright but road and scenes are dark without being sufficiently illuminated. No color visible on road. Entire view becomes dark with camera auto-exposure.
6. Rainy (20)	Dark illumination, low sensitivity of camera. Some cannot be separated from overcast. We look at wiper on/off to decide rainy state. Wet surface has specular reflection of scenes and sky.
7. Direct light (13)	Sun at front with glare in image. Even hard for human driver to see

	road. May have highlight on road surface.
8. Snowy (1)	Snow intervene the scene and camera, makes image noisy. Road sides are more snow-covered than road.
9. Fog (5)	A half-transparent layer in front of camera blurs scenes. Camera exposure can enhance contrast.
10. Night (55)	Night is tagged when vehicle headlights are on. It includes rural night without street light, city with street light, and wet ground with strong reflection of other car lights and city lights

2.3 Data Mining with Driving Video

The huge driving video archive contains rich accident moments, traffic patterns, and other environment related aspects, which are statistically meaningful to conclude the reasons of crashes from environment, vehicle, and driving behavior. We first compute the probability distributions of all the parameters extracted from a large number of video clips. Crash data will then be located in the distributions to visualize the general trends of accidents and most frequent crashes. Data mining is applied to determine the most crucial factors and generate vehicle crash testing scenarios for various areas, weather conditions, traffic flows, collision speeds and distances.

The first effort we have done is the data mining of road appearance under the influence of weather and illumination. This work uses the unsupervised learning to cluster visual features in different weather and illuminations. 360 video clips with 324k locations are collected evenly over different seasons, weathers, and time. We find possible clusters of videos by K-mean algorithm including their centroids, variations, and inter-cluster distances. The features used are average intensity, chroma, and variation from four regions of sky, road, left and right roadsides in the video frame as shown in Fig. 6. We do not use Hue as feature since it is more related to the roadside materials other than weather. We use Chroma instead of Saturation because saturation has a singular value when intensity is zero. Figure 11 shows the distribution of features mentioned above in each clusters human tagged.

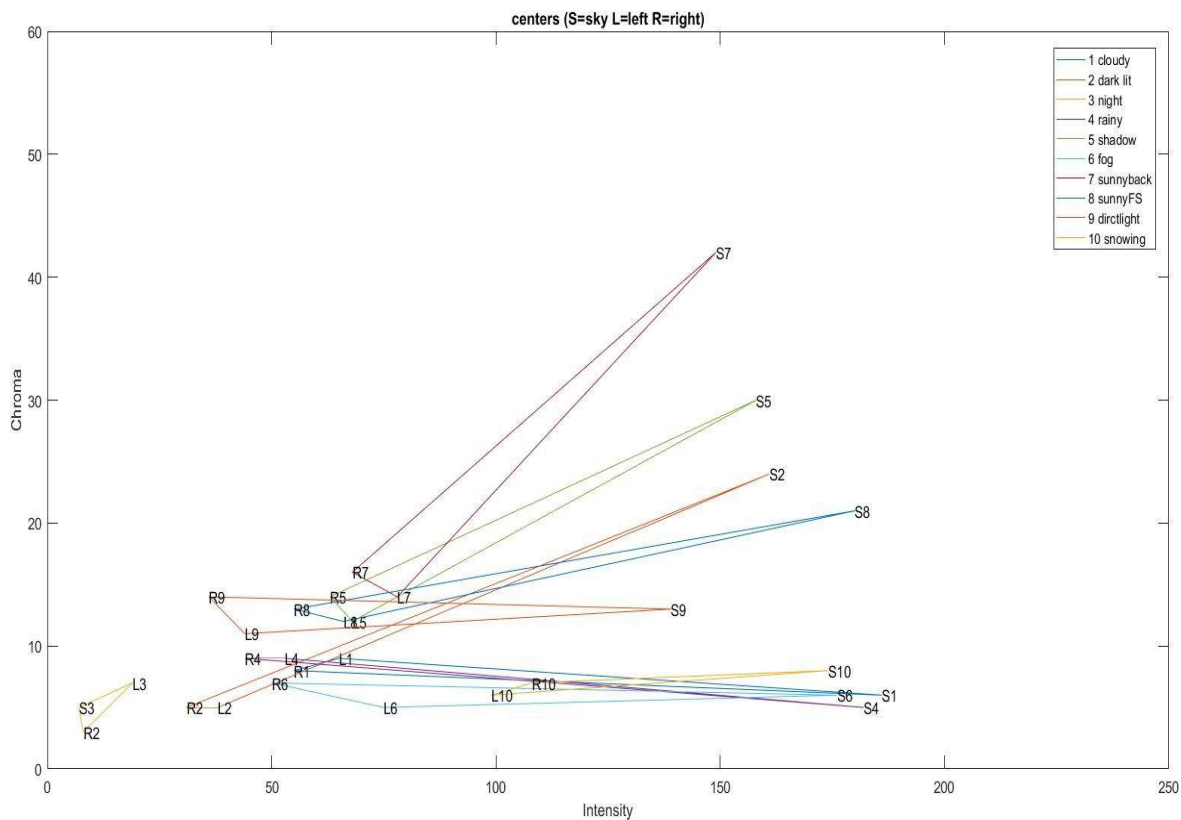


Fig. 11 Visualization of weather/illumination categories tagged by humans in intensity (horizontal) and chroma (vertical) space. Triangles indicate those parameters from sky, left and right roadside regions. The intensity and chroma of sky is more significant than left and right roadsides. We can also notice the similarity among fog, cloudy, rainy, and snowy.

By looking at category C_i tagged by humans with averaged features in four regions, we can generate typical views of all categories in Fig. 12. Because manual tagging of shadow is at clip level other than detailed to frames, it contains many sunny frames. The shadow average is like that of sunny back to the sun. Raining and cloudy are much similar in nature in human tagging, because the wiper movement is ignored in averaging colors in the road profiles. This tagging may also miss some small sets of weathers like urban night or even with wet ground.

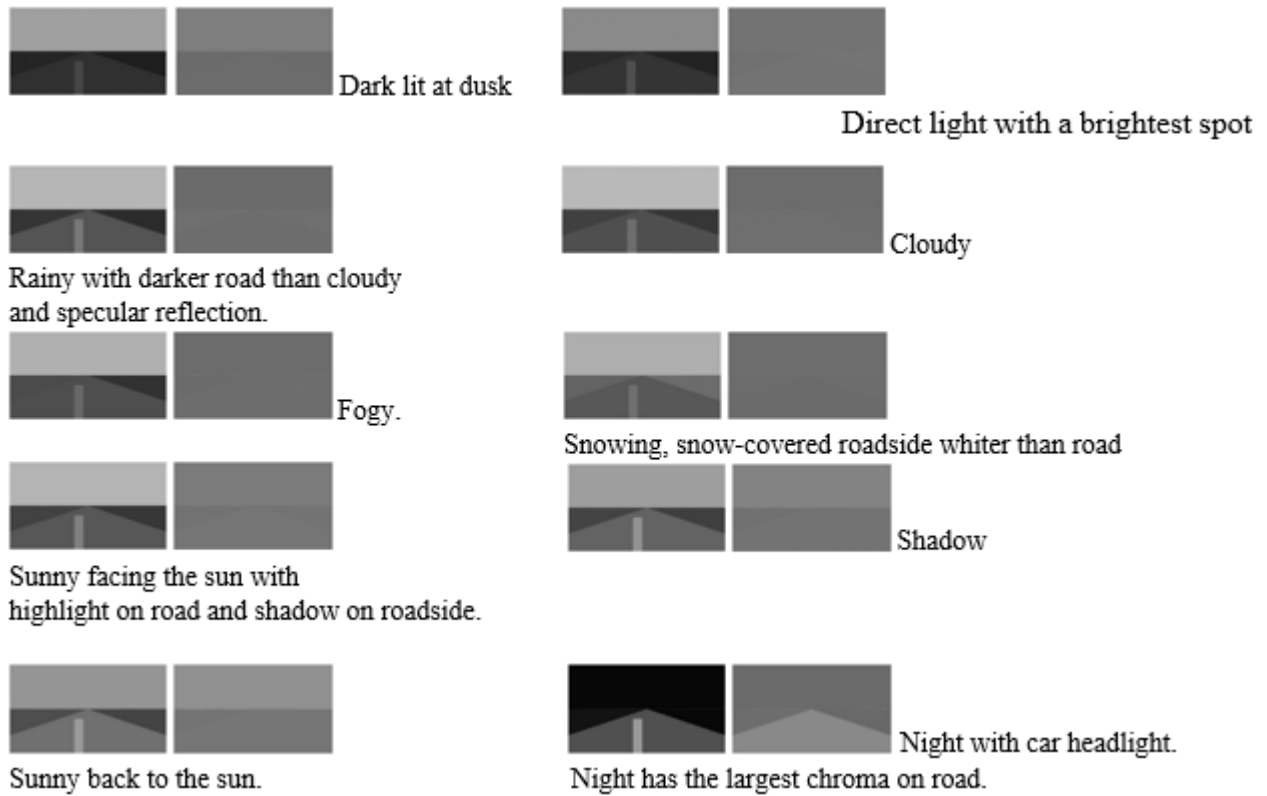


Fig. 12 Intensity and chroma average pairs in human tagged categories. The central vertical bars on road indicate the color variation against surface due to specular reflection, shadow, surface repairing, etc. Compare to the intensity, chroma averages are much smaller (displayed with 10% scale up).

Because human tagging is intuitive and qualitative at clip level, we further apply K-means algorithm on all 324k frames to find quantitative results of weather and illumination clusters S_j . K-means is selected because the weather properties are of continuous nature rather than discrete samples. We also calculate likelihood probability $P(S_j|C_i)$ to find out which human tagged categories contribute to each cluster the most. The dominant category is used to name the cluster as a related name. For a cluster without any major category contributing to it, it is considered as an outlier. K-mean clusters are clear and non-overlapped partition of the feature space, but are not necessarily consistent to the human tagged categories exactly. Moreover, we compare the clusters (Fig. 13) to the human tagged categories in Fig. 11 with triangles from average image intensity and chroma in the three regions.

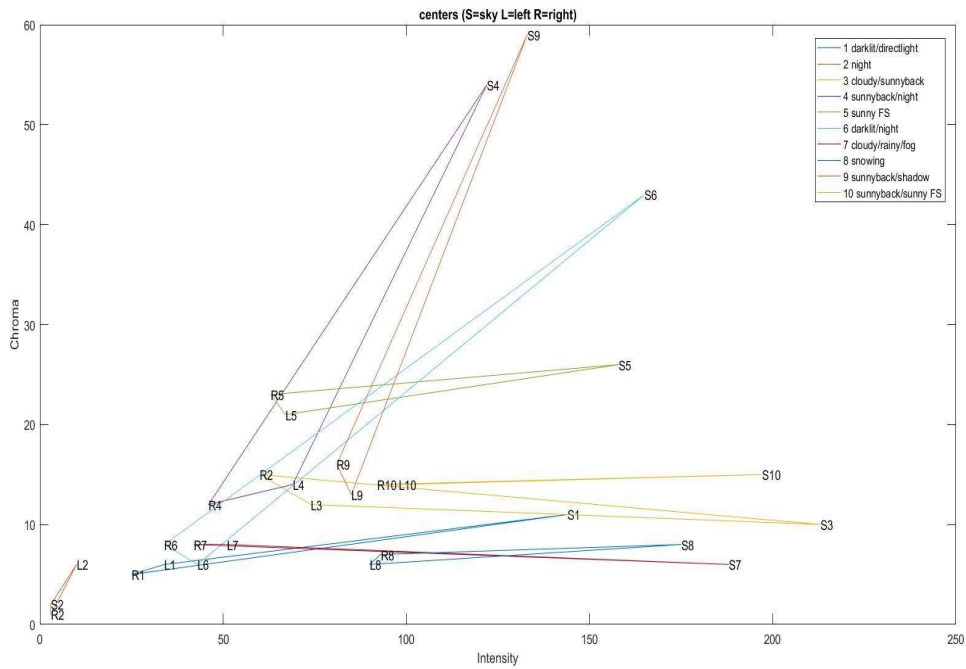


Fig. 13 Visualization of weather/illumination clusters (K=10) from K-means algorithm with intensity (horizontal) and chroma (vertical) space. It has a sparser inter-distance between weather clusters.

To examine the cluster structure in various levels of details, we change the number of clusters $K=10, 9, \dots, 2$ to obtain different clusters $S_j, j=1, \dots, K$. By comparing $P(S_i)$, a K-mean tree is generated as in Fig. 14. This tree tells a way to summarize weather and illumination clusters from coarse to fine levels using their related names at each K . Night is always the most distinct cluster to separate from daytime. Figure 15 is the result when cluster number is set to 7. On the other hand, we have also increased K in clustering. The raining and cloudy are unable to be separated up to $K=30$. This indicates that rainy and cloudy are unable to be separated clearly if observation is not down to the level of raindrop. The typical views of the clusters for $K=10, 7, 3$ are also visualized in Fig. 16 by using centroid values of K-mean clusters; their values are consistent across different K . For $K=3$, views are separated to night, bright, and dark daytime, in which dark road is researched in road edge detection recently. With a coarse clustering, the intra-class distances become larger, meaning such classes have larger variations.

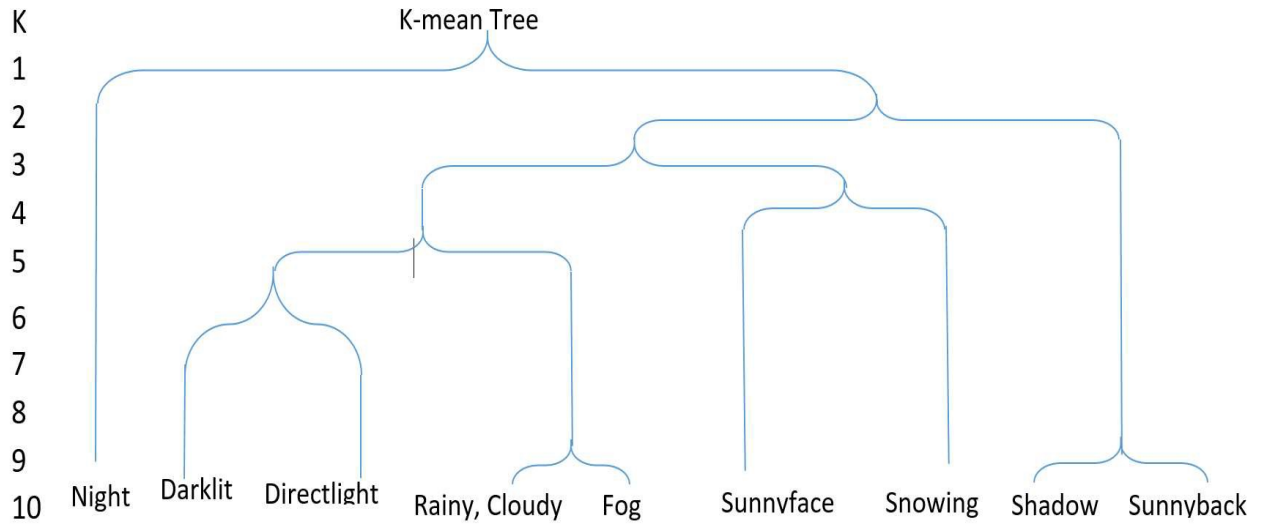


Fig. 14 K-means tree containing a hierarchy of clusters for different K, obtained from analysis of $P(S|C)$ for each K.

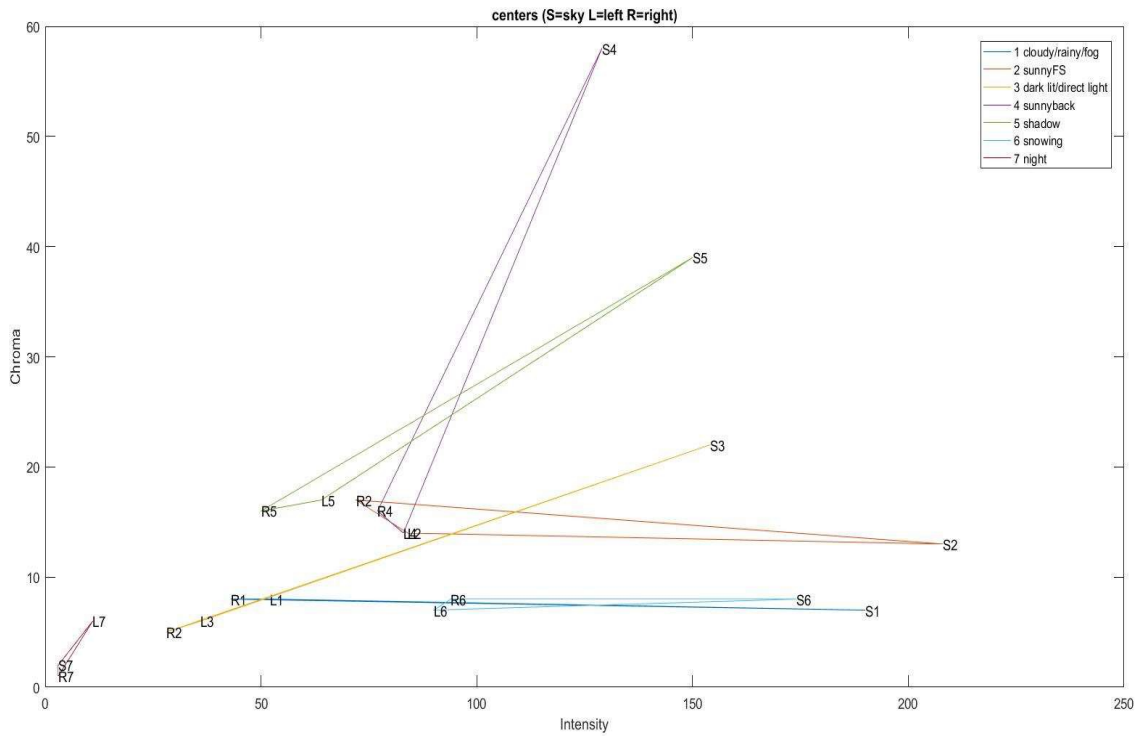


Figure 15 Visualization of weather/illumination clusters ($K=7$) from K-means with intensity (horizontal) and chroma (vertical) space.

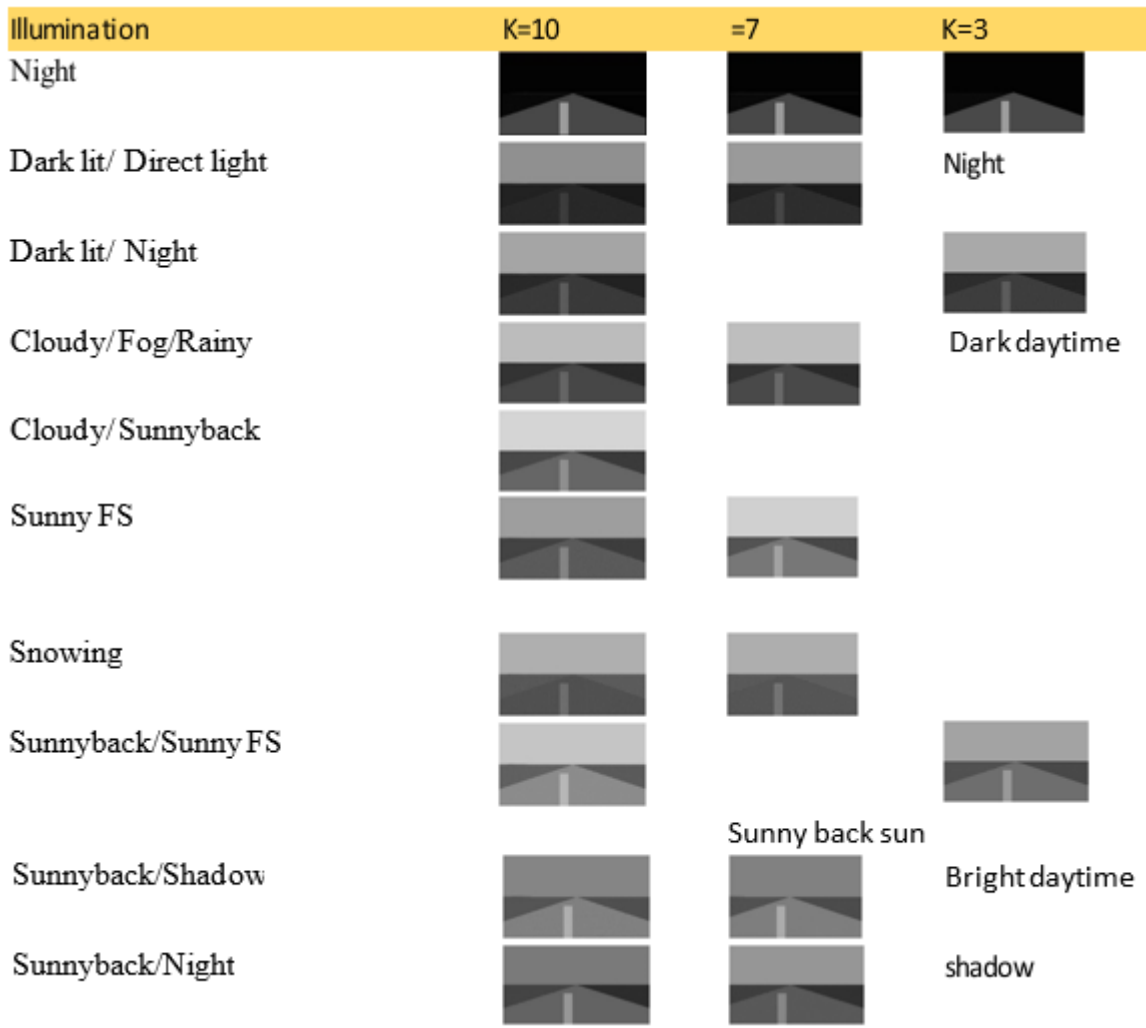


Fig. 16 Typical views of clustered weathers in intensity for $K = 10, 7,$ and 3 clusters. Central bars are standard deviation from the road average color.

The ultimate goal of weather/illumination clustering is the recognition of weather in video frames for the guidance of road edge detection. Based on learned weather clusters, we classify another larger set of video containing 300 clips. The same regions and parameters are extracted from each frame. The distances of a frame to previously obtained cluster centroids are computed in the feature space to find the closest cluster. Note that K-means is a different division of feature space based on equal distance, while human tagging is more qualitative on visual properties even if the measure is imprecise.

In the weather and illumination classification, the results for $K=7$ is obtained at frame level for verification using the road profiles. Table II shows the consistency measure of the classification

as compared to the human tagged labels. For each cluster, we assign it with a related category name mentioned above. If human tagged category name is the same in a frame, the frame is consistent; otherwise, it is counted inconsistent. The cluster-wised consistency rates are thus obtained after evaluating another 60 video clips \times 9k frames in a testing set different from the training set. We found some inconstancy from the passing or front vehicles in the road profiles. Again, this is the evaluation via human tagging, which is not an absolute measure because of its ambiguity.

This results show how roads look like under full spectrum of weather and illuminations based on mining large driving videos. The clustering of weather sensitive data results in stable clusters without overlap in the feature space, as compared to ambiguous human weather tagging. The classification based on learned clusters can help weather identification in video frames [16], and be applied to road edge detection or invisibility declaration in locating road edges [17].

From the video mining, we have observations: (1) White lane marks are the most reliable features to follow. Painting lane mark is an inexpensive way to improve infrastructure for autonomous driving. (2) Road edges may be invisible in poor weather and illumination conditions. Providing wrong edges to the vehicle control will cause even worse consequences. Human drivers memorize road, follow front car, or refer to scenes on roadside in such maneuver. (3) The data mining discriminates different weather, rather than recover the absolute illuminance values as auto-exposure cameras are used.

TABLE II Matching rates of weather and illumination labels between human perception and data clustering

	C1	C2	C3	C4	C5	C6	C7	%
	cloudy/rainy /fog	Sunny facing the sun	dark lit/ direct light	Sunny back to the sun	shadow	snowing	night	
K=7	93%	80%	91%	87%	80%	96%	98%	90%

3. RESULTS

The followings are the papers published after the project is funded. All of them uses driving video in the analysis and several of them are data mining of driving video. The constructed online video database facilitates these studies because these videos can be accessed by multiple users online. The large video volumes also provided many variations of road scenarios and appearances to test and evaluate our designed algorithms and software for safety driving.

M. Kilicarslan, J. Y. Zheng, A. Algarni, Pedestrian detection from non-smooth motion, IEEE Intelligent Vehicle, 487-492, 2015.

M. Kilicarslan, J. Y. Zheng, Bridge motion to collision alarming using driving video, 23th International Conference on Pattern Recognition, 1870-1875, 2016.

M. Kilicarslan, J. Y. Zheng, K. Raptis, Pedestrian detection from motion, 23th International Conference on Pattern Recognition, 1857-1863, 2016.

Z. Wang, J. Y. Zheng, M. Kilicarslan, Visualizing road appearance properties in driving video. Nicograph Internal 2016. 25-28.

M. Kilicarslan, J. Y. Zheng, Direct vehicle collision detection from motion in driving video, IEEE Intelligent Vehicles, 2017, 1558-1564.

C. Liu, R. Fujishiro, L. Christopher, J. Y. Zheng, Vehicle-bicyclist dynamic position extracted from naturalistic driving videos, IEEE Transactions on Intelligent Transportation Systems, 18(4), 734-742, 2017.

Z. Wang, G. Cheng, J. Y. Zheng, All weather road edge identification based on driving video mining. IEEE Intelligent Transportation Systems Conference, 1-6, 2017.

G. Cheng, Z. Wang, J. Y. Zheng, Big-video mining of road appearances in full spectrums of weather and illuminations, IEEE Intelligent Transportation Systems Conference, 1-6, 2017.

In an updated version to investigate the road environment, we further produce road profiles from vehicle passed roads to visualize appearances of road over miles. This is used in the project of road edge detection under various weather and illumination conditions. Figure 17 shows another display of videos on Cloud to host thousands of video clips. Figure 18 is the video clip page possible to tag visual properties on roads.

http://roadpr...56065&page=70 | Video - 2851 | Video - 2849 | http://roadprof...eo_gallery.php | Video - 2720

roadprofiles.cs.iupui.edu/video_gallery.php

Gallery | Users | Tags | Help | Admin Panel

Categories

- Logoff
- My Videos
- Recent Videos

Search Videos

Video Number : Search video

Video Number Between: Start num End num

Date is Exactly: yyyy-mm-dd

Dates Between: yyyy-mm-dd yyyy-mm-dd

On Road Components:

Off Road Components:

Light Condition:

Submit Query

Videos

Videos in database: 7389

« 0 1 2 3 4 5 6 7 8 9 10 »

#1 #2 #3

#4 #5 #6

#7 #8 #9

#10 #11 #12

« 0 1 2 3 4 5 6 7 8 9 10 »

RoadProfiles is a production of Computer Science
© IUPUI.EDU

Figure 17 Video database visualized in a site for road appearance investigation under different weather and illumination conditions.


http://roa...65&page=70 | Video - 2851 | Video - 2849 | http://road...e=13&cat=0 | Video - 162 | Video - 2720

roadprofiles.cs.iupui.edu/video.php?vid=b12e65ca-2123-11e6-8b6b-001aa0506f47&title=162

Gallery | Users | Tags | Help | Admin Panel

Prev Video | Next Video

Video: 162



Download Video
Delete

On-Road Materials:
 Asphalt: New Old Repaired
 Concrete
 Gravel
 Wet
 Snow Covered
 Unassigned
 Multiple


Off-Road Materials:
 Grass: Green Yellow/Gray
 Vegetation: Green Yellow Gray
 Trees/Forest: Green Black/Dark
 Gravel
 Concrete/Curb
 Ditch/Cliff
 Guardrail/Cones
 Snow Covered
 Unassigned
 Multiple

Weather / Illumination:
 Sunny: Facing sun Sun at the back
 Shadow
 Cloudy
 Dark Lit
 Night
 Direct Light
 Snowing
 Rainy
 Fog
 Bad Windshield
 Unassigned
 Multiple

Segments:
 --no segments found--


submit

Key Frame:



Video Summary
 Video Name: 0240032612165800073.MOV
 Road Materials: unassigned
 Off-Road Materials: unassigned
 Light Condition: unassigned
 Unassigned: 1
 Last Modified: 2016-05-23 16:19:46
 Segments: 0
 Video Num: 162
 UploadedBy: jjang zheng

Profile Info.



Feature.

Figure 18 Video clip displayed with road profile, attributes, key frames and video.

4. DISCUSSION

Using the video analysis software developed above, close to 50 attributes such as vehicle speed, turning angle, vehicle location, target distance and motion, surrounding traffic, and so on can be extracted as a feature vector from each video clip and the associated GPS record. For data classes such as crash, near miss, and safe driving, supervised machine learning methods will find their most dominant and deterministic parameters with the probability distributions. Statistical procedures such as PCA and ICA will be used in the parameter sorting. Clusters will be obtained for describing crash accidents by using K-means clustering algorithm. Any new video clip uploaded to the web database will be classified into above classes by comparing its feature vector with the learned accident cluster in order to predict and evaluate real and near miss crashes. This can also guide the development of vision and sensor based vehicle onboard crash avoidance technique. The clusters further indicate the vehicle testing scenarios with the highest priority.

5. ACKNOWLEDGMENTS

This work is supported by UTC OSU mini-project grant during 2014-2016, and is also supported by the Department of Computer Science, Indiana University Purdue University Indianapolis.

REFERENCES

1. M Kilicaslan, JY Zheng, Visualizing driving video in temporal profile, IEEE Intelligent Vehicle Symposium, 2014, 1-7.
2. A Jazayeri, H Cai, JY Zheng, M Tuceryan, Vehicle detection and tracking in car video based on motion model, IEEE Transactions on Intelligent Transportation Systems, 12 (2), 583-595.
3. M Kilicaslan, JY Zheng, Towards collision alarming based on visual motion, 15th IEEE Int. Conf. Intelligent Transportation Systems (ITSC), 2012, 654-659.
4. Y Kai, EY Du, EJ Delp, J Pingge, J Feng, C Yaobin, R Sherony, and H Takahashi, An Extreme Learning Machine-based pedestrian detection method, IEEE Intelligent Vehicles Symposium (IV), 2013, 1404-1409
5. S Wang, S Luo, Y Huang, JY Zheng, P Dai, Q Han, Railroad online: acquiring and visualizing route panoramas of rail scenes, The Visual Computer, 2013, 1-13.
6. S Wang, JY Zheng, S Luo, X Luo, Y Huang, D Gao, Route panorama acquisition and rendering for high-speed railway monitoring, IEEE International Conference on Multimedia and Expo (ICME), 2013, 1-6.
7. RE Gamage, A Joshi, JY Zheng, M Tuceryan, A high resolution 3D tire and footprint impression acquisition for forensics applications, IEEE Workshop on Applications of Computer Vision (WACV), 2013, 317-322.
8. H Cai, JY Zheng, Automatic heterogeneous video summarization in temporal profile, 21st International Conference on Pattern Recognition (ICPR), 2012, 2796-2800.
9. H Cai, JY Zheng, Video anatomy: cutting video volume for profile, 19th ACM International Conference on Multimedia, 1065-1068, 2011.
10. M. Kilicaslan, J. Y. Zheng, A. Algarni, Pedestrian detection from non-smooth motion, IEEE Intelligent Vehicle, 487-492, 2015.
11. M. Kilicaslan, J. Y. Zheng, Bridge motion to collision alarming using driving video, 23th International Conference on Pattern Recognition, 1870-1875, 2016.
12. M. Kilicaslan, J. Y. Zheng, K. Raptis, Pedestrian detection from motion, 23th International Conference on Pattern Recognition, 1857-1863, 2016.
13. Z. Wang, J. Y. Zheng, M. Kilicaslan, Visualizing road appearance properties in driving video. Nicograph Internal 2016. 25-28.
14. M. Kilicaslan, J. Y. Zheng, Direct vehicle collision detection from motion in driving video, IEEE Intelligent Vehicles, 2017, 1558-1564.
15. C. Liu, R. Fujishiro, L. Christopher, J. Y. Zheng, Vehicle-bicyclist dynamic position extracted from naturalistic driving videos, IEEE Transactions on Intelligent Transportation Systems, 18(4), 734-742, 2017.
16. Z. Wang, G. Cheng, J. Y. Zheng, All weather road edge identification based on driving video mining. IEEE Intelligent Transportation Systems Conference, 1-6, 2017.
17. G. Cheng, Z. Wang, J. Y. Zheng, Big-video mining of road appearances in full spectrums of weather and illuminations, IEEE Intelligent Transport

Safety Implications of Traffic Dynamics in Congested Freeway Traffic

Sub-Project PI: Prof. B. Coiffman

CEEGS

OSU

Safety Implications of Traffic Dynamics in Congested Freeway Traffic

Accomplishments:

This research has focused on driver behavior in the presence of large speed differentials between lanes. Results have found that drivers' car-following behavior not only depends on the lead vehicle in their lane, but also the speed of the adjacent lane. It turns out that these dependencies can also emerge in seemingly free flow traffic. Specifically, when traveling next to a slow-moving lane some drivers will choose a free speed below the speed limit. This new-found regime will help advance our understanding of how congested traffic can really a mix of queued and non-queued traffic, and thus, having the potential to exhibit properties of both states.

Impact: The findings enumerated in the accomplishments section are important because most car-following models strictly depend on the leader in the same lane as the follower. So this work has found a previously unrecognized dependency. These findings should eventually lead to more robust microscopic traffic flow models, which in turn will improve the performance of all applications that depend on these models (from safety applications, to traffic control, to urban planning).

Products:

Journal articles:

Ponnu, B., Coifman, B., "Speed-Spacing Dependency on Relative Speed from the Adjacent Lane: New Insights for Car Following Models," *Transportation Research Part B*. Vol 82, 2015, pp 74-90.

Ponnu, B., Coifman, B. "When Adjacent Lane Dependencies Dominate the Uncongested Regime of the Fundamental Relationship," *Transportation Research Part B*. Vol. 104, 2017, pp 602-615.

Conference papers:

Ponnu, B., Coifman, B., "Speed-Spacing Dependency on Relative Speed from the Adjacent Lane: Presenting New Insights for Car Following Models" *Proc. of the 96th Annual Meeting of the Transportation Research Board*, 2017.

Ponnu, B., Coifman, B. "When Adjacent Lane Dependencies Dominate the Uncongested Regime of the Fundamental Relationship- Abridged," [in review] *Proc. of the 97th Annual Meeting of the Transportation Research Board*, 2018.

Smart Cities: A Simple Framework for On-Demand Mobility Services

Sub Project PI's: Prof. U. Ozguner, Prof. K. Redmill

Smart Cities: A Simple Framework for On-Demand Mobility Services

An effort was undertaken to develop slow-moving platforms (single-person or 4-people vehicles) that would provide transportation for the mobility-impaired in a smart city. The effort has been initiated by the City of Columbus and later supported by an NSF Project (through its CPS: Smart Cities Program). Within this small sub-project we investigated the computer-communication architecture needed to establish such a service and considered the “crash imminent” situations between pedestrians and vehicles.

Products: Two vehicles were developed for a demonstration.

Collaboration: City of Columbus, NSF.

Impact: This project provides an opportunity to investigate Crash Imminent scenarios for slow-moving platforms in dense pedestrian environments and related human factor issues. It also provides an opportunity to deal with the legal and administrative aspects of autonomous vehicle deployment, albeit in a traffic environment different than roadways.

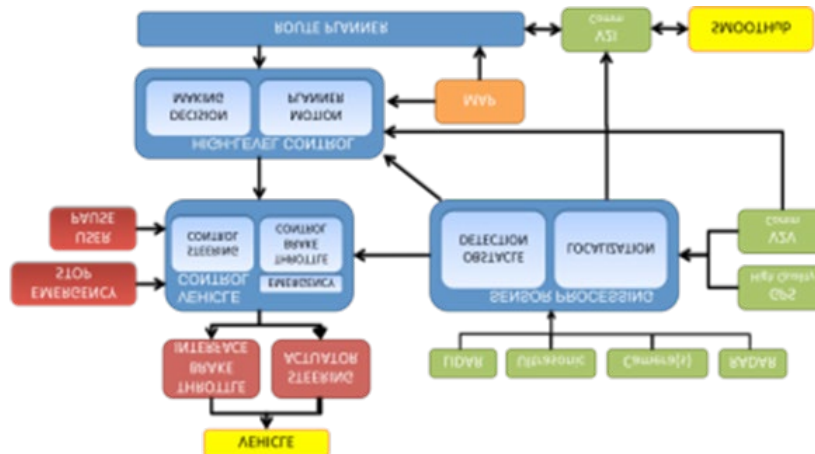
This study builds up on earlier work conducted at The Ohio State University on passenger and pedestrian motion and behavior models for public transportation applications within Intelligent Transportation Systems (ITS). Detecting and tracking the motion of pedestrians around intelligent vehicles become more important as partial and full autonomy applications are developed for heavily populated urban environments. Motion models capturing the behavior of pedestrians around a vehicle, or even predicting future trajectories for vehicle path planning will improve transportation safety immensely.

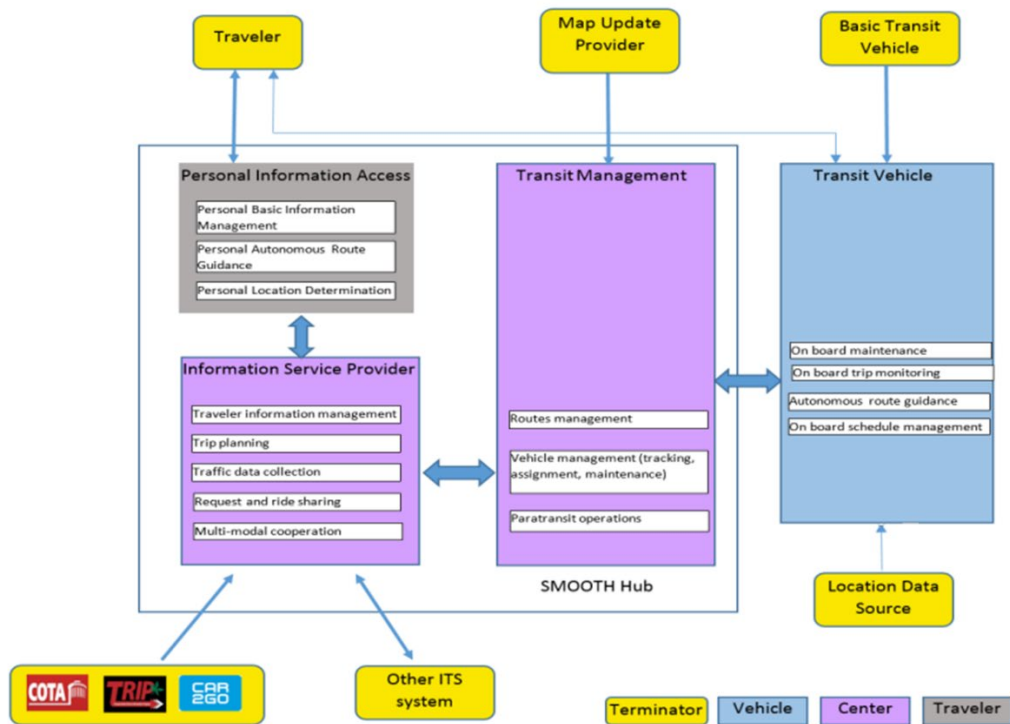
Challenge:

- Most people in the US do not live or work close to a transportation stop –first mile / last mile problem
- Walking does not apply to everybody -elderly people, handicapped people, people with luggage
- Elderly people are expected to become 20% of the entire US population in 25 years

Solution:

- On demand automated shuttles
- Smartphone app used for reserving space in an automated shuttle
- Shuttle timing has to be coordinated with the bus arrival and departure
- Connected Vehicle technology (intersection safety, cooperative driving)





Problems in “Dense, pedestrian-rich” environments

- It is difficult to predict trajectories of pedestrians, due to highly dynamical movement of pedestrians and crowd traffic: sidewalks, pedestrian crossing
- “Collision imminent” (pedestrian in front of vehicle) check is not sufficient.

We will be continuing our investigations supported through other funding sources.